



## Review article

# Overview of continuum and particle dynamics methods for mechanical modeling of contractional geologic structures



Gary G. Gray<sup>a,\*</sup>, Julia K. Morgan<sup>b</sup>, Pablo F. Sanz<sup>a</sup>

<sup>a</sup> ExxonMobil Upstream Research Company, P.O. Box 2198, Houston, TX 77252-28189, USA

<sup>b</sup> Rice University, Dept. Earth Science, Houston, TX 77005, USA

## ARTICLE INFO

*Article history:*

Received 29 October 2012

Received in revised form

23 November 2013

Accepted 30 November 2013

Available online 12 December 2013

*Keywords:*

Structural modeling

Finite element

Particle dynamics

Discrete element

Boundary element

Finite difference

Constitutive laws

Contractional structures

Plasticity

## ABSTRACT

Mechanically-based numerical modeling is a powerful tool for investigating fundamental processes associated with the formation and evolution of both large and small-scale geologic structures. Such methods are complementary with traditional geometrically-based cross-section analysis tools, as they enable mechanical validation of geometric interpretations. A variety of numerical methods are now widely used, and readily accessible to both expert and novice. We provide an overview of the two main classes of methods used for geologic studies: continuum methods (finite element, finite difference, boundary element), which divide the model into elements to calculate a system of equations to solve for both stress and strain behavior; and particle dynamics methods, which rely on the interactions between discrete particles to define the aggregate behavior of the system. The complex constitutive behaviors, large displacements, and prevalence of discontinuities in geologic systems, pose unique challenges for the modeler. The two classes of methods address these issues differently; e.g., continuum methods allow the user to input prescribed constitutive laws for the modeled materials, whereas the constitutive behavior 'emerges' from particle dynamics methods. Sample rheologies, case studies and comparative models are presented to demonstrate the methodologies and opportunities for future modelers.

© 2013 Elsevier Ltd. All rights reserved.

## 1. Introduction

Forward mechanical modeling has become an increasingly popular tool in the study of structural geology, as it can provide fundamental insights into the formation, evolution, and geometries of complex geologic features. In this paper, we present an overview of the current state of mechanical modeling as applied to the structural geology of contractional systems. We focus on methods receiving the majority of usage today, specifically, finite elements and particle dynamics. Finite difference and boundary element techniques are briefly described for comparison. This paper is targeted at the general structural geology community, and assumes only minimal experience with numerical modeling and the concepts behind the different techniques. It is not possible to review the entirety of numerical structural modeling in a short paper, as this topic encompasses scales from the entire crust and lithosphere down to initiation and growth of a single fracture. Therefore, we focus this review on the application of forward mechanical

modeling of contractional systems, from the regional cross-section to the individual structure scale, similar to the scale of problems addressed by balanced section analysis.

Many modeling techniques commonly used by the geologic community were developed for solving engineering problems. The goal of most engineering applications is to determine the stress/strain conditions at which a system or structure begins to fail. Such problems range from soil stability for foundation analysis to metal fatigue for bridges, airplane, and automotive parts. It is typically less important for the structural engineer to understand the behavior of the model system once failure is underway (i.e., the behavior of a foundation after it cracks or the airplane wing as it tears and falls off). Most such codes are optimized for these types of low-strain, failure-limit analysis problems. Geologists, of course, are typically more interested in the evolution of systems after the onset of failure. For example, folds and faults begin to form and move, permanently changing the state of the system. These types of geologic behaviors are kinematically discontinuous in nature, and generally involve large displacements and strains, conditions for which few engineering codes are optimized. The accumulation of large strains causes excessive distortion of the mesh used in continuum modeling, preventing such models from converging on a solution. These issues pose unique challenges that must be

\* Corresponding author. Current address: Rice University, Dept. Earth Science, Houston, TX 77005, USA.

E-mail addresses: [graybeau@sbcglobal.net](mailto:graybeau@sbcglobal.net), [ggg2@rice.edu](mailto:ggg2@rice.edu) (G.G. Gray).

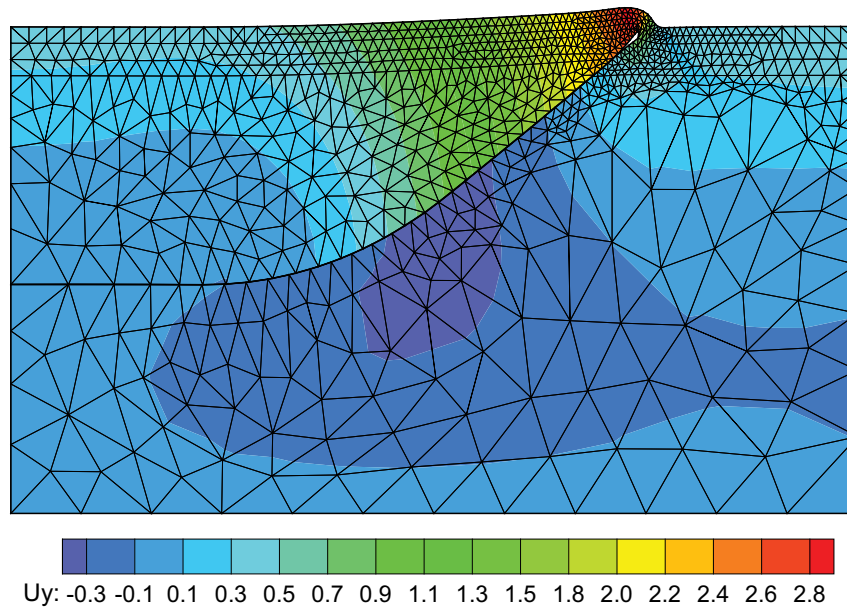


**Fig. 1.** Diagram showing a typical finite element model with the mesh and a pre-defined slip surface. This view shows the model after significant lateral contraction. Colors are contours of displacement in the vertical direction. Modified from Sanz (2008).

overcome when modeling discontinuous processes, such as faulting, with many of these methods (Munjiza, 2004).

Despite these cautionary comments regarding the abilities of forward mechanical modeling in structural geology, numerical models offer powerful ways to identify and assess feasible solutions to structural interpretations, and provide important insights into the mechanical conditions under which they must form. For these reasons, forward modeling is becoming increasingly popular, rapidly advancing the state of knowledge in structural studies with a wide range of applications.

## 2. Continuum and particle-based numerical methods

Numerical methods are required to study geologic problems that are too complex for simple analytical solutions. The linear momentum balance law is the governing equation for the deformation of solids and these methods are capable of solving this equation in problems with irregular geometries and boundaries, and non-linear material behavior. The mechanical behavior of geologic materials can be modeled as a continuous mass or as discrete particles. A spectrum of different modeling approaches have been developed for wide variety of applications. The following section examines the most common continuum and discrete numerical methods utilized in forward modeling of contractional geologic structures.

### 2.1. Continuum methods

The basic strategy of the continuum methods (finite element, finite difference, and boundary element) is to discretize the model geometry into smaller subdomains (e. g., Laursen and Simo, 1993, and many others). The subdomains share nodes and edges, and any surfaces that are defined within the model. The nodes, edges and surfaces comprise a mesh that provides the framework within which the calculations are made (Fig. 1). The models runs are divided into a series of time-steps. At each time-step, the mesh is moved by pre-defined loads and/or displacements at the model boundaries, and the effect of these changes on adjacent nodes and

elements propagates via a system of mathematical equations throughout the rest of the mesh as needed to maintain equilibrium.

Continuum methods assume that the processes and properties being modeled can be represented as smoothly varying fields. The three methods discussed herein deal with this continuum in different ways. Finite element and finite difference models use a similar meshing strategy for the entire domain. The primary distinction between these two techniques is that the finite element method solves an equivalent weighted-integral, or weak form of the problem (e.g., Zienkiewicz, et al., 2005). The finite difference method directly approximates the partial differential equation, or strong form of the problem, using finite difference equations (e.g., Detournay and Hart, 1999). The finite element approach is generally better suited for non-linear problems with irregular geometries and complex boundary conditions. In addition, there are many well-developed and verified academic and commercial finite element codes with large capacities in terms of computing power and material complexities. For these reasons, it is the most widely applied numerical method for modeling in structural geology (Melosh and Williams, 1989; Mäkel and Walters, 1993; Braun and Sambridge, 1994; Erickson and Jamison, 1995; Mohapatra and Johnson, 1998; Smart et al., 1999; Cardozo et al., 2003; Ellis et al., 2004; Kwon and Mitra, 2004; Panian and Wiltschko, 2004; Crook et al., 2006b; Sanz et al., 2007; Simpson, 2009; Albertz and Lingrey, 2012; Albertz and Sanz, 2012; see also Table 1).

The finite difference method is the oldest member in this family of numerical methods. This method transforms the original partial differential equations into systems of algebraic equations with unknowns at the grid points. As with the finite element method, the solution of the system of equations is obtained after imposing the necessary initial and boundary conditions. Finite difference methods are excellent for static problems such as heat flow and temperature modeling, and have some strong adherents for lithospheric-scale viscous models (e.g., Gerya, 2010).

A commonly used finite difference code for geologic structures is FLAC (Fast Lagrangian Analysis of Continua) (<http://www.itascacg.com/flac/overview.html>), first released in 1986. FLAC utilizes an explicit integration scheme and considers large strains (geometric nonlinearities) in the solution. An important advantage

**Table 1**

Compilation of continuum structural modeling studies showing the methods and constitutive behaviors.

Author/s, year	Method, program	2D/3D	Material model
Melosh and Williams, 1989	FEM	2D	Elastic layer
Mäkel and Walters, 1993	FEM	2D	Drucker–Prager with non-associated flow
Poliakov et al., 1993	FD	2D	Mohr–Coulomb with non-associative and viscous rheologies
Erickson, 1995	FEM	2D	Drucker–Prager with associated flow
Erickson and Jamison, 1995	FEM	2D	Drucker–Prager and viscous rheologies
Willemsse et al., 1996	BEM	3D	Linear elastic
Barnichon and Charlier, 1996	FEM, LAGAMINE	2D	Drucker–Prager and Van Eekelen non-associative flows
Jamison, 1996	FEM, SAVFEM	2D	Coulomb friction (faults) and viscous rheology
Cooke and Pollard, 1997	BEM	2D	Linear elastic
Sassi and Faure, 1997	FEM	2D	Linear elasticity and elasto-plasticity; Coulomb friction contact
Strayer and Hudleston, 1997	FD, FLAC	2D	Mohr–Coulomb
Upton, 1998	FD, FLAC	2D	Mohr–Coulomb with non-associative flow
Mohapatra and Johnson, 1998	FEM	2D	Linear elastic
Gerbault et al., 1998	FD, FLAC	2D	Mohr–Coulomb
Niño et al., 1998	FD, FLAC	2D	Drucker–Prager and viscous rheologies
Maerten et al., 1999	BEM, POLY3D	3D	Linear elastic
Smart et al., 1999	FEM, JAC2D	2D	Elasto plastic
Vanbrabant et al., 1999	FEM, ADELI	2D	Drucker–Prager (2-invariant)
Beekman et al., 2000	FEM, TECTON*	2D	Mohr–Coulomb (no hardening)
Cooke et al., 2000	BEM	2D	Linear elastic
Cooke and Underwood, 2001	BEM, FRIC2D	2D	Linear elastic
Erickson et al., 2001	FD, FLAC	2D	Linear elasticity and Mohr–Coulomb
Strayer et al., 2001	FD, FLAC	2D	Mohr–Coulomb with non-associative flow
Schultz-Ela, 2002	FEM, GEOSIM-2D	2D	Drucker–Prager with non-associative flow and softening
Cardozo et al., 2003	FEM, ABAQUS	2D	Drucker–Prager with associative and non-associative flow
Guiton et al., 2003a	FEM	3D	Elastoplastic with diffuse inherited weak discontinuities (anisotropic)
Guiton et al., 2003b	FEM	3D	Mohr–Coulomb with multiple internal variables
Savage and Cooke, 2003	BEM, POLY3D	3D	Linear elastic
Wissing and Pfiffner, 2003	FEM, MICROFEM	2D	Mohr–Coulomb with viscosity
Ellis et al., 2004	FEM	2D	Mohr–Coulomb with non-associated flow and strain softening
Erickson et al., 2004	FD, FLAC	2D	Mohr–Coulomb with non-associative flow and cohesion softening
Kwon and Mitra, 2004	FEM, MARC-MENTAT	3D	Elastoplastic power law
Savage and Cooke, 2004	BEM, POLY3D	3D	Elastic, and frictionless faults
Bellahsen et al., 2006	BEM, POLY3D	3D	Linear elastic
Crook et al., 2006a, b	FEM, ELFEN	2D	Critical State Model (SR3)
Henk, 2006	FEM, ANSYS	2D	Elastic perfectly plastic; power law creep
Sheldon et al., 2006	FD, FLAC3D	2D	Cam Clay with associative flow
Simpson, 2006	FEM	2D	Elasto-visco-plastic
Couples et al., 2007	FEM, SAVFEM	2D	Drucker–Prager with Non-associative flow
Fiore et al., 2007	BEM, POLY3D	3D	Linear elastic
Stockmal et al., 2007	FEM	2D	Drucker–Prager with softening and viscous flow
Sanz et al., 2007	FEM, SPIN2D	2D	Coulomb friction, elasticity and Matsuoka-Nakai
Wilkins, 2007	BEM, POLY3D	3D	Linear elastic
González et al., 2008	FD, PARAVOZ/FLAC	2D	Mohr–Coulomb, non-associative, no dilation
Maniatis and Hampel, 2008	FEM, ABAQUS	3D	Elastic and viscoelastic
Sanz, 2008	FEM, SPIN2D	2D	Coulomb friction, elasticity and Matsuoka-Nakai
Simpson, 2009	FEM	2D	Mohr–Coulomb visco-elasto-plastic
Smart et al., 2009	FEM, ABAQUS	2D	Mohr–Coulomb with non-associative flow
Resor and Flodin, 2010	FEM, ABAQUS	2D	Linear elastic
Smart et al., 2010	FEM, ABAQUS	2D	Mohr–Coulomb with non-associative flow
Simpson, 2011	FEM	2D	Mohr–Coulomb with non-associative flow
Albertz and Lingrey, 2012	FEM, ELFEN	2D	Critical State Model (SR3)
Albertz and Sanz, 2012	FEM, ELFEN	2D	Critical State Model (SR3)
Nollet et al., 2012	FEM, ELFEN	2D	Critical State Model (SR3)
Resor and Pollard, 2012	BEM, TWODD	2D	Linear elastic
Smart et al., 2012	FEM, ABAQUS	2D	Mohr–Coulomb with non-associative flow

of the explicit formulation is that it employs a very simple solution algorithm. The major drawback of the explicit formulation is the restriction to keep the time-steps small (i.e. to divide the model run into a large number of calculation time-steps) to assure that the solution is numerically stable. FLAC overcomes this drawback to some extent by utilizing automatic inertia scaling and automatic damping. Examples of the use of finite difference method in solving structural problems can be found in Poliakov et al. (1993), Strayer and Hudleston (1997), Upton (1998); Gerbault et al. (1998), Niño et al. (1998); Erickson et al. (2001), Strayer et al. (2004), Sheldon et al. (2006), González et al. (2008), and Gerya (2010).

The boundary element technique differs from the other continuum methods in that only certain “boundaries” within the

model are gridded (e.g., Thomas, 1993). Typically, these key boundaries are the faults within a model, not the physical edges of the model (Fig. 2). The rest of the model consists of a virtual box surrounding the faults. The box is set up to apply stresses in both the horizontal and vertical directions, and the azimuth of these applied loads can be easily varied. A solution is computed at the boundaries within the model, which can then be propagated to any point or surface within the interior of the virtual box. These models are restricted to using linear elasticity as the material model and small deformation analysis for the kinematics because the method solves an exact linear solution of the governing partial differential equations (Bregbia and Dominguez, 1989). This constraint greatly reduces the time it takes to run a model, by decreasing the number

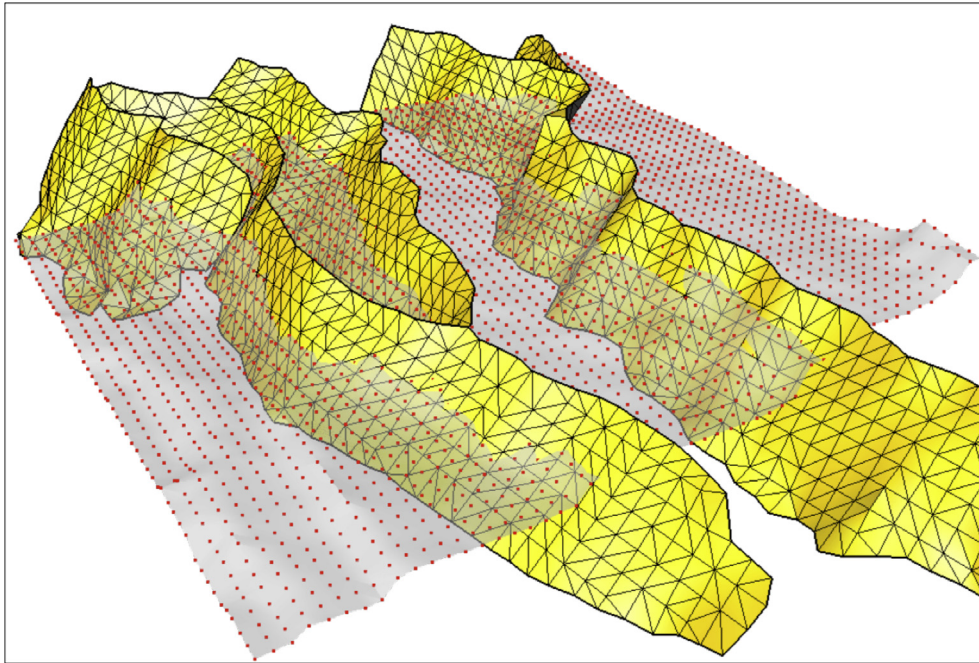


**Fig. 2.** An example boundary element model showing that the faults are the only meshed regions within the model. The initial solution is calculated on this mesh. The dotted surface represents a stratigraphic horizon that provides a set of loci for propagating the calculated values away from the fault mesh, but does not participate in the calculated solution. The edges of the dotted surface roughly coincide with the lateral edges of the 'virtual box' described in the text. The top and base of this box coincide essentially with the top and bottom edges of the faults. From Maerten et al. (2002).

of time-steps required to achieve a solution. This type of problem is well suited to modeling the elastic interactions (i.e. stress patterns) between faults or other discontinuities within a medium, as long as strains remain relatively small. The use of the boundary element technique in structural geology has been popularized largely through the work of Thomas (1993), Cooke and Pollard (1997), Savage and Cooke (2003, 2004), Maerten, et al. (2006), Hilley (et al., 2010), and the Stanford Rock Fracture Project through the development of the Poly 3D program.

## 2.2. Particle dynamics

Particle dynamics techniques define another modeling approach that is becoming increasingly used for simulating the evolution of geologic structures (e.g., Saltzer and Pollard, 1992; Burbidge and Braun, 2002; Strayer and Suppe, 2002; Finch et al., 2004; Cardozo et al., 2005) (Fig. 3). The broad class of particle dynamic techniques includes the discrete element method (Cundall and Strack, 1979), lattice-solid method, (Mora and Place, 1993), and the contact dynamics method, (Radjaï and Dubois, 2011). Particle dynamics techniques were adapted from molecular dynamics and utilize particles rather than mesh elements (Allen and Tildesley, 1987; Walton, 1984; Place and Mora, 1999). Thus, these techniques fall into a class referred to as "mesh-free numerical methods" (Li and Liu, 2004). The particles are distinct from one another, and a continuum of properties between particles is not required. Each particle is assigned material properties (e.g., size, density, elastic moduli, etc.) and inter-particle properties (e.g., friction, various bond properties such as shear and tensile strengths, etc.) (Fig. 3). Particle interactions and resultant forces are calculated and updated in a pairwise fashion throughout the simulation. Particle accelerations, velocities, and displacements are calculated for each system state using Newton's first equation of motion. Particles can be circular (in 2D), cylindrical or spherical (in 3D), or other shapes (elliptical, angular, superquadrics) (e.g.,

Rothenburg and Bathurst, 1992; Ting et al., 1993; Lin and Ng, 1997; Cundall, 1971; Hart et al., 1988; Williams and Pentland, 1991), but circles and spheres allow for the simplest contact detection (Cundall and Strack, 1979; PFC<sup>2D</sup>, 1999; Allen and Tildesley, 1987). The overall behavior of the system is determined by the interparticle force-displacement laws, which can include hard-sphere, soft-sphere, non-linear attractive-repulsive laws, among others (Allen and Tildesley, 1987; Li and Liu, 2004). One attraction of using distinct particles is that discontinuities can initiate and evolve naturally during a model run (so-called emergent behavior). Also, particle displacements and associated strains are unlimited, because mesh distortion is not an issue. And although particle properties and interactions are distinct, it is possible to calculate a composite continuum for any volume for comparison with natural materials (Cundall and Strack, 1983; Thornton and Barnes, 1986; Oda and Iwashita, 1999; Morgan and McGovern, 2005b).

The discrete nature of particle dynamics methods also poses unique challenges. One issue is the computational effort required to track all particles and their multiple interactions. This concern typically limits the size of simulations, and therefore the resolution of many modeled systems, as computational effort (and time) scales approximately linearly with the number of particles. This issue has been largely overcome, however, through efficient bookkeeping schemes and the development of parallel computational methods (e.g., Plimpton, 1995; Plimpton and Hendrickson, 1996; Munjiza, 2004). A second issue, like with the finite difference method, is the small time-steps required to maintain system stability. The critical time-step for particle translation is proportional to the square root of the ratio of particle mass to particle stiffness, (Cundall and Strack, 1979; Walton, 1984; Oda and Iwashita, 1999; PFC<sup>2D</sup>, 1999). Thus, the dynamics of the smallest particle in the system greatly influences model run-time. The size of the simulation time-step also depends on expected particle velocities, because displacements are integrated linearly. Time-steps must be chosen to ensure that particle displacements are small

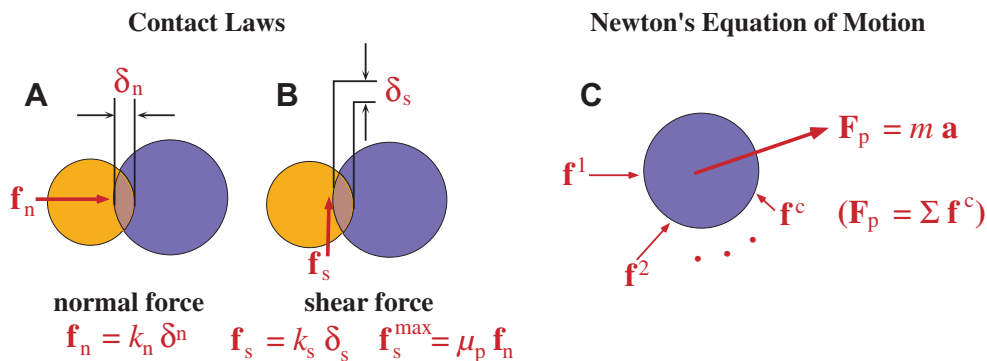


**Fig. 3.** Simplified Particle Dynamics methodology. (A) Particles in normal contact experience elastic resistance as a function of their relative distance (numerical overlap). (B) Particles in shear contact experience elastic resistance as a function of their relative shear displacement, with an upper limit defined by interparticle friction. (C) Contact forces acting on a given particle are summed at the particle centroid, yielding a centroid force that can be used to solve for acceleration and new particle positions. Force-displacement relationships can be linear or non-linear.

enough for all incremental interparticle forces to be detected, otherwise instability can occur. This imposes a more fundamental limit on time-step size that cannot be overcome via advances in computational speed.

Another fundamental challenge for particle dynamics models is the need to constrain independently the bulk constitutive properties of an assemblage, as these are not defined *a priori* as for continuum models. The overall behavior of the system is determined by the aggregate effects of all interparticle interactions, which depend on the myriad of properties noted above. Proper implementation of particle dynamics methods, therefore, requires careful characterization of the bulk material properties, including mechanical strength, elastic moduli, contractive/dilatative behavior, and more, under a range of stress paths and strain histories. These bulk properties should also be related and tuned to natural materials to the degree possible. Approaches and examples used to address this need are discussed further below.

The application of particle dynamics-type modeling to contractional geologic systems has a relatively short history, and is still undergoing substantial development. The initial application of particle dynamics modeling (using disks or spheres) to geomaterials was in soil mechanics (Cundall and Strack, 1979) and granular flow (Walton, 1984), but the approach proved to be useful for examining a variety of geologic processes ranging from the deformation of fault gouge (Morgan and Boettcher, 1999; Aharonov and Sparks, 2004; Guo and Morgan, 2006, 2007; Abe and Mair, 2005), clay smear (Egholm et al., 2008), volcanic spreading (e.g., Morgan and McGovern, 2005a,b; McGovern and Morgan, 2009), caldera collapse (Hardy, 2008), and extension, contraction, and indentation (e.g., Yamada and Matsuoka, 2005). Recent simulations of contractional systems demonstrate the potential of this method for forward mechanical modeling of complex tectonic systems. For example, Naylor et al. (2005) carried out 2D simulations of doubly vergent wedges. Hardy et al. (2009) examined the detailed processes of fault initiation and linkage within doubly vergent wedges. Miyakawa et al. (2010) investigated the effects of spatially varying friction on formation of the out-of-sequence faults and accretionary wedge slope breaks. These detailed investigations build upon a series of earlier studies that introduced the capabilities of the method for large-scale geodynamic modeling as well as study of discrete structures (e.g., Vietor, 2003; Burbidge and Braun, 2002; Finch et al., 2004; Strayer and Suppe, 2002; Strayer et al., 2004; Cardozo et al., 2005; Benesh et al., 2007).

One appealing aspect of particle dynamics modeling is that the discrete nature of the particular assemblage effectively reproduces the phenomenology of natural or laboratory systems, which are also composed of discrete or breakable materials. For example,

specific configurations and load paths can be generated to reproduce all of the constitutive behaviors reviewed below (e.g., elasticity, plasticity, etc.), and the accompanying changes in volume. Thus, particle dynamics models can provide unique insights into the micromechanics associated with these observed behaviors (Trent et al., 1987; Morgan and Boettcher, 1999; Morgan, 1999, 2004; Aharonov and Sparks, 2004; Potyondy and Cundall, 2004), whereas this is not possible when the constitutive behavior is a model input.

Many of the limitations of all the techniques discussed in this paper are constrained by our ability to make millions of calculations in a rapid manner. More complex behaviors will be achievable at larger and larger scales as computing power continues to rise.

### 3. Constitutive laws for mechanical models

Constitutive models of geologic materials are equations that relate the stresses that arise in the model to the resulting deformation of the body. The stress–strain behavior of natural geologic materials is complex and dependent on the loading path, and the most advanced constitutive laws retain and reflect the strain history of the materials in all parts of the model (e.g., Crook et al., 2006a, b; Albertz and Sanz, 2012). Sedimentary rocks, in particular, can undergo spectacular increases in strength as they age, largely due to a decreasing volume during consolidation (tracked by porosity), but also due to physical and chemical changes (diagenesis) (e.g., Jones and Addis, 1986; Jones, 1994; Karig and Morgan, 1994; Albertz and Sanz, 2012). Overall, rocks are discontinuous, anisotropic, and inelastic, giving rise to complex and non-linear behavior (Harrison and Hudson, 2000; Jaeger et al., 2007). A great variety of continuum- and particle-based constitutive models are commonly employed for geologic materials. In the following section, some of the most useful and commonly applied constitutive models are described together with their limitations.

#### 3.1. Linear elasticity

The simplest constitutive relationship commonly used in numerical modeling is linear elasticity. This relationship is based upon Hooke's law, which for a simple spring can be written:

$$F = kx$$

An applied force ( $F$ ), compresses the spring a distance ( $x$ ) based upon the value of the spring constant ( $k$ ). The spring returns to its initial state when the force is removed, therefore all strain accumulated is reversible, or recoverable. There is no 'memory' of the

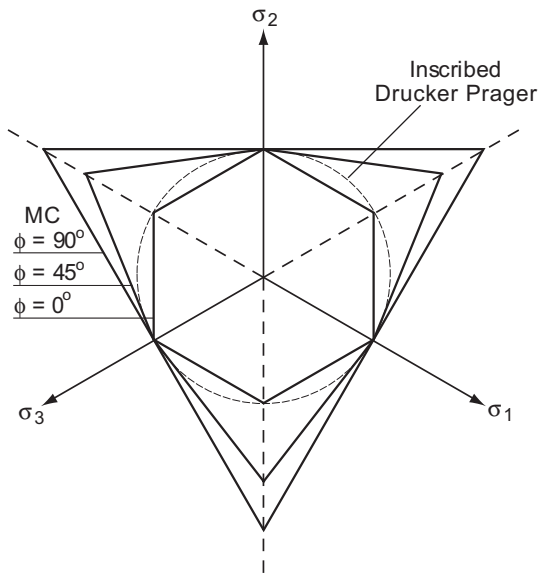


**Fig. 4.** Cross-sectional shape of the yield curves for 3 Mohr–Coulomb and 1 Drucker–Prager material on deviatoric plane. The Mohr–Coulomb materials correspond to internal friction angles of 0, 45, and 90°. The angular nature of the failure surface is obvious, and presents difficulties in computation. The Drucker–Prager yield surface is tangent to all of the Mohr–Coulomb surfaces at the major stress axes, but is a smooth circle, and much more computationally stable. (Modified from Sanz, 2008).

strain history, nor is there a failure criterion. Linear elasticity is employed in some 2D and all 3D structural restoration software (e.g., Maerten and Maerten, 2006; Guzowski et al., 2009). This property allows programs such as Dynel and Kine-3D to easily map results between the restored and deformed states (Maerten and Maerten, 2006; Guzowski et al., 2009; Durand-Riard et al., 2013), which is a key benefit of these analyses. Linear elastic behavior is also integral to the boundary element technique. The use of elasticity in this technique facilitates the ease of calculation, which

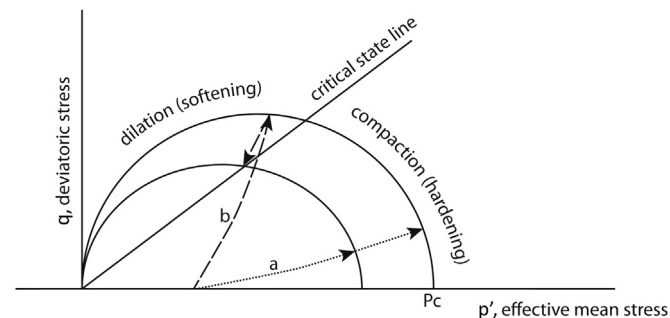


**Fig. 5.** The basic features of a critical state material model, showing the complex, non-linear behavior of geologic materials.  $p$  is the effective mean stress, and  $q$  is the deviatoric stress.  $P_c$  is the preconsolidation pressure. The ellipsoidal curves starting at the origin are failure envelopes. The critical state line divides regions of differing failure regimes. Right of this line, failure is compactional, and results in decreasing porosity and strengthening of the material. Left of this line, failure is dilatational and weakens the material. If a rock experiences stress trajectory (a), it will hit the smaller failure envelope in the hardening part of the curve. This will result in compactive failure (strengthening), which will move the envelope outward. If this stronger rock is then subjected to stress trajectory (b), it will hit the outer failure envelope on the dilatational part of the curve. The material will weaken, and the stresses will drop along the steep short downward trajectory until the stresses hit the critical state line. If the stress path continues to reside at failure, the envelope will continue to shrink. If the deviatoric stress drops, however, then the failure envelope in this example will have shrunk back to its original, smaller size. Diagenesis (cementation) also strengthens the rock and works to move the failure envelope outward. The intersection of the failure envelope with the origin reflects that this material has no cohesion or tensile strength.

allows quick testing of many scenarios (e.g., Shamir and Eyal, 1995; Brebbia and Dominguez, 1989; Melosh and Williams, 1989; Willemse et al., 1996; Cooke and Pollard, 1997; Cooke et al., 2000; Resor and Flodin, 2010; Resor and Pollard, 2012). The major drawback of using this material behavior is that geological structures are mostly the result of permanent, non-recoverable (i.e., inelastic) deformation. A second drawback is the lack of a failure criterion so there is no limit to the stresses that can arise during deformation. Even so, elasticity will provide an approximation for basic, low-strain problems in structural geology. Elastic-based models may even be able to capture the strain field for large deformation problems with the appropriate displacement boundary conditions.

### 3.2. Plasticity

Materials for which a permanent deformation remains after loading and unloading are called plastic materials (Hill, 1950). Many materials exhibit an elastic behavior up to their yield stress, and undergo plastic deformation when loaded beyond the yield stress, and are thus called elasto-plastic materials. As described in more detail below, geologic materials are often modeled with pressure-sensitive elasto-plastic rate-independent material laws (e.g., Mandl, 1990), as this type of material model is capable of capturing four fundamental behaviors: (i) recoverable elastic strain (ii) inelastic strain upon yield (iii) cohesive–frictional strength dependent on loading path, and (iv) stiffness deterioration during plastic deformation. This combination of behaviors captures the essence of rock deformation (Jaeger et al., 2007), and is a good approximation for many geologic applications.

Mathematically, plasticity models have three major ingredients: (1) a yield function or criterion for the onset of inelastic deformation, (2) a flow rule and plastic potential function to determine the plastic strain rate, and (3) a hardening/softening law that governs the evolution of the yield function. The general characteristics of the yield function can be appreciated by its cross-sectional shape on a deviatoric plane (Fig. 4) and by its trace on a meridian or  $p$ – $q$  plane (Figs. 5 and 6). The  $p$ – $q$  plane highlights the variable yield stress as a function of the mean effective stress. The deviatoric plane is perpendicular to the isotropic line ( $p$ -axis) and to any meridian plane.

The flow rule for a material is governed by a property called the plastic potential. The plastic potential is a curving surface, and can be superimposed over the failure surface, as in Fig. 7. If the plastic potential surface is parallel to the failure envelope at the point of failure, then the flow rule is called associative. If they are not parallel, then the flow rules are called non-associative. Associative and non-associative plastic flow rules are employed to help mimic the behavior of geologic materials (Erickson and Jamison, 1995; Sheldon et al., 2006; Mäkel and Walters, 1993; Poliakov et al., 1993; Strayer et al., 2004; Cardozo et al., 2003; Crook et al., 2006a; Albertz and Sanz, 2012). An associative behavior over-predicts dilatancy during shear failure (Drucker and Prager, 1952; Bolton, 1986; Goodman, 1989) and therefore is generally not appropriate for most geo-materials. It can be a reasonable approximation for the deformation of geologic materials undergoing plastic compaction, however. Non-associative flow rules provide more flexibility to capture the inelastic volume change (dilative or compactive) during different plastic loading (shearing or compaction).

#### 3.2.1. Mohr–Coulomb

Most geologists are familiar with the Mohr–Coulomb failure criterion. This model, first proposed as a method to predict soil strength for engineering purposes (Coulomb, 1773), defines the

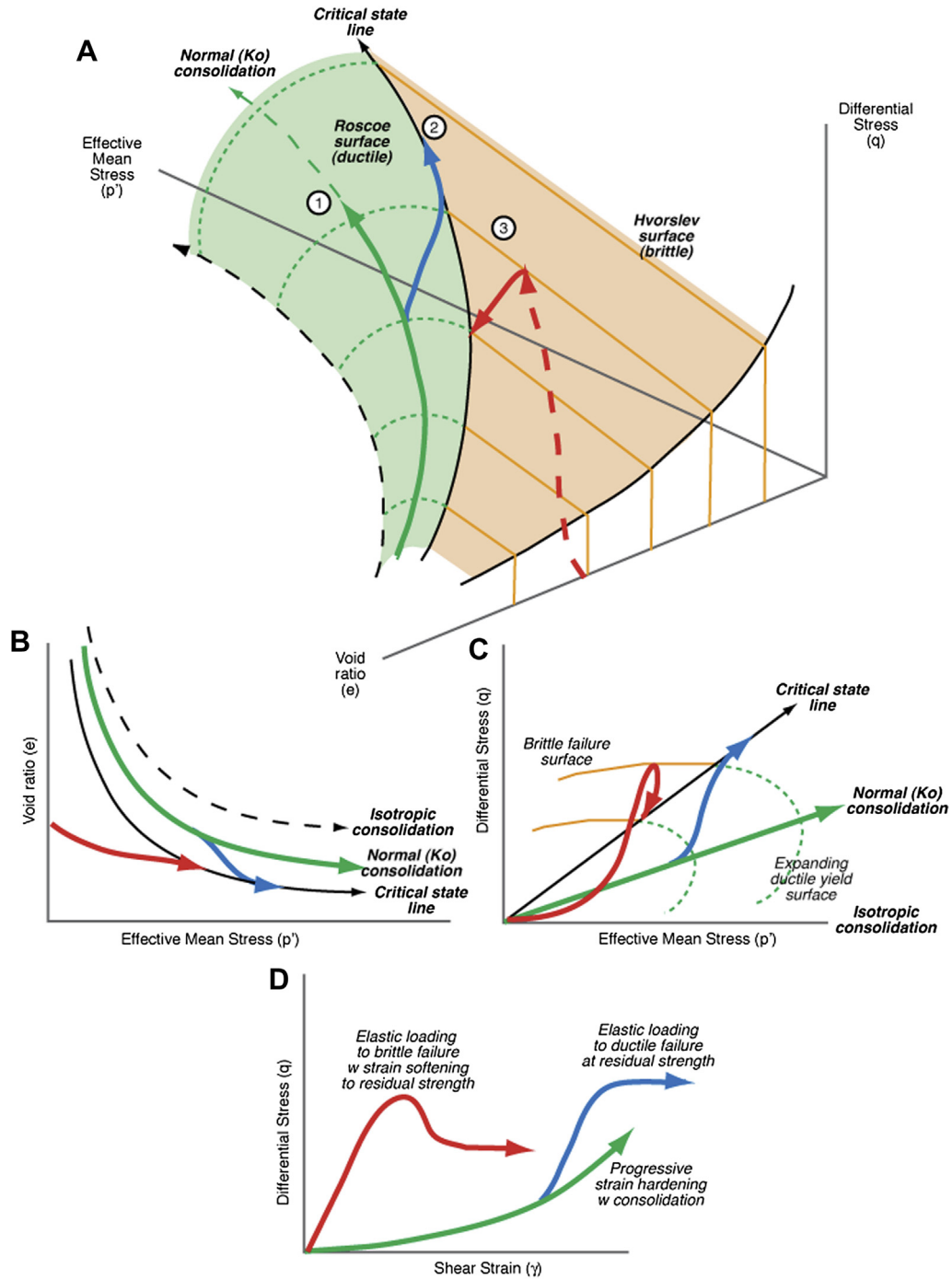


**Fig. 6.** Representative stress paths and yield surfaces for natural sediments and rocks, based on the critical state model (Muir Wood, 1990). (A) Three dimensional yield surface plotted in  $p'$ - $q$ - $e$  space, showing the strong dependence of rock strength on void ratio (or porosity). Three stress paths are shown: (1) uniaxial consolidation, which results in progressive compaction at decreasing rates with increasing  $p'$ ; (2) compactive shear loading following uniaxial consolidation, to the point of ductile failure (critical state); (3) dilative shear loading from no differential stress (i.e., overconsolidated state), accommodated by elastic deformation to brittle failure, followed by strain softening to residual frictional sliding (at critical state) along the fracture. (B) Changes in void ratio (volume) for the three stress paths. (C) Projections of stress paths in  $p'$ - $q$  space, showing yield surface for given void ratio section. (D) Typical differential stress–strain plots for given stress paths, showing (1) progressive strain hardening, (2) compactive shear deformation to residual strength, and (3) dilative shear deformation to residual strength.

shear strength of a material as a linear function of the effective normal stress acting on the failure surface (Fig. 7):

$$\tau_f = c + \sigma_n \tan \phi,$$

where  $\tau_f$  is the shear strength,  $c$  is the cohesion,  $\sigma_n$  is the effective normal stress on the shear plane, and  $\phi$  is the friction angle (Mohr, 1900, 1914).

Mohr–Coulomb is a classical plasticity model that accounts for the shape of the failure surface on the deviatoric plane. It is widely used for representing the yield and failure behavior of cohesive-frictional materials. This model has the shape of an irregular hexagon on the deviatoric plane (Fig. 4) and predicts a higher yield/failure strength in compression than in extension as observed in geomaterials (Fig. 7). On a meridian plane as in Fig. 7, the shape of the yield/failure criterion is a straight line for a constant value of the

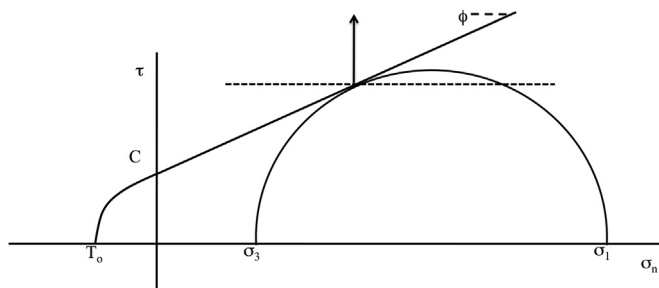


**Fig. 7.** Basic elements of the Mohr circle (Mohr, 1900, 1914). Normal stress ( $s_n$ ) and shear stress ( $t$ ) are plotted on the  $x$ - and  $y$ -axes, respectively.  $s_1$  and  $s_3$  are the minimum and maximum principle stresses.  $\Phi$  is the slope of the failure surface, also known as the angle of internal friction,  $C$  is the cohesion and  $T_0$  is the tensile strength. The failure envelope, from  $T_0$  through  $C$  and along  $\Phi$ , is the combined Coulomb–Griffith failure criterion. When stress conditions cause the Mohr circle to become tangent to the Coulomb failure criterion, an additional parameter, the plastic potential function, can be defined. This function describes the flow behavior after failure. In this case, the plastic potential function and the failure surface are not parallel, so the flow law is termed non-associated. If the two were parallel, the flow law would be associated. The horizontal plastic potential surface defines flow along the direction of the arrow, resulting in isochoric, or constant volume deformation. If the plastic potential were parallel to the failure criterion, and the arrow were to have a negative slope in  $\tau$ - $\sigma$  space, deformational flow would be highly dilatational.

friction angle, which may not be realistic for some cohesive-frictional materials. This failure criterion has been equipped with different flow rules and hardening/softening laws to model the evolution of geologic structures (Griffith, 1921; Poliakov et al., 1993; Strayer and Hudleston, 1997; Upton, 1998; Gerbault et al., 1998; Beekman et al., 2000; Strayer et al., 2004; Guiton et al., 2003a; Wissing and Pfiffner, 2003; González et al., 2008; Simpson, 2009; Smart et al., 2009).

The appeal of the Mohr–Coulomb description is that it is a simple formulation, it predicts a limit to material strength based on applied stresses, and it provides geometric constraints for the failure planes. The main weakness of the Mohr–Coulomb model, compared to more sophisticated constitutive laws, is its inability to capture compactive plastic deformation (Potts and Zdravkovic, 1999). Mohr–Coulomb behavior is relatively easy to implement numerically for two-dimensional loading conditions. The corners within the yield surface in three dimensions, however, make it less straightforward to implement, as discussed below. Moreover, these models do not account for the influence of the intermediate principal stress, which could be significant for some rocks (Mogi, 1967; Colmenares and Zoback, 2002; Morris and Ferrill, 2009). Thorough

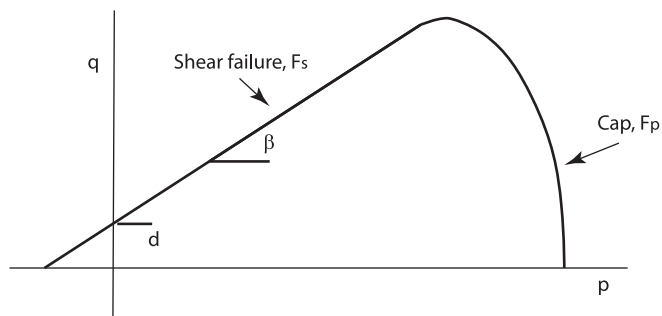


**Fig. 8.** Basic elements of the modified Drucker–Prager constitutive model in  $p$ – $q$  space. The shear failure line,  $F_s$ , with angle  $\beta$  is directly analogous to the friction angle in the Mohr–Coulomb model. The key differences in this implementation is the addition of an end cap,  $F_p$ , that allows for compactive failure, and provision for both tensile strength (failure surface left of  $y$  axis) and cohesion ( $d$ ). Modified from Abaqus 6.11 User Documentation (2012).

reviews of the Mohr–Coulomb law can be found in many sources, including Timoshenko and Goodier (1970), Parry (2004), and Jaeger et al. (2007).

### 3.2.2. Drucker–Prager

Drucker and Prager (1952) proposed a pressure-dependent plasticity failure criterion similar to Mohr–Coulomb. This two-invariant failure criterion, written in terms of the deviatoric and mean effective stresses is:

$$q = a + bp$$

where  $q$  is the deviatoric stress,  $p$  is the effective mean stress, and  $a$  and  $b$  are cohesion-like and friction-like material constants.

The original Drucker–Prager model was developed to capture shear failure, therefore is also poorly suited to accommodate compactive failure (Jaeger et al., 2007). The original two-invariant Drucker–Prager model also did not capture the higher yield/failure strength in compression than in extension as observed in most geologic materials. An advantage of the Drucker–Prager model is that the two-invariant yield surface plots as a smooth circular cone centered on the isotropic line in principal stress space, as opposed to the angular yield surface for Mohr–Coulomb (Fig. 4). This single smooth function of the stresses is differentiable everywhere due to the absence of corners. The Drucker–Prager model has been modified to add an ‘end cap’ to better represent compactive plastic deformation (Drucker et al., 1957) and the failure surface has been moved to include cohesive and tensile behavior (Fig. 8). In this enhanced implementation, Drucker–Prager model is transitional between Mohr–Coulomb and critical state soil mechanics-type material descriptions presented below, and has been featured in several structural modeling studies (e.g., Mäkel and Walters, 1993; Erickson and Jamison, 1995; Barnichon and Charlier, 1996; Erickson, 1993; Niño et al., 1998; Vanbrabant et al., 1999; Schultz-Ela, 2002; Cardozo et al., 2003; Stockmal et al., 2007).

### 3.2.3. Critical state theory

Critical state models were originally developed for cohesionless soils (Roscoe et al., 1958; Schofield and Wroth, 1968) but have been also applied to concrete (Chen, 1982) and rocks (Gerogiannopoulos and Brown, 1978). Critical state theory considers that granular media, when continuously sheared, reach a state in which shearing occurs without changes in differential stresses, or volume and porosity. Critical state theory is defined in terms of effective mean stress ( $p$ ), differential stress ( $q$ ), and porosity or void ratio ( $e$ ), which captures volumetric changes (Muir Wood, 1990). Two-dimensional depictions of critical-state yield criteria are shown in Figs. 5 and 6, highlighting the interdependence of mean and differential stress. Fig. 6 conveys a generalized three-dimensional yield surface and representative stress paths within that surface. The different components of the critical state model provide descriptions for a much wider range of material behaviors, including cohesive–frictional strength, compaction, dilatancy, strain hardening–softening, and non-associated plastic flow (see also Atkinson and Bransby, 1978; Muir Wood, 1990). Each behavior is predicted by where the stress path intersects the failure surface (Figs. 5 and 6).

The original critical state models do not capture the cohesive and tensile behavior observed in cemented soils and rocks (Fig. 5). In addition, the yield criterion is often described using a two-invariant formulation like the basic Drucker–Prager model. Critical state models have been refined by extending the yield surface into the tensile region and by introducing an asymmetric yield surface that more closely approximates experimentally determined failure characteristics (Crook et al., 2006a). Several recent articles present aspects of these modified critical state models for forward

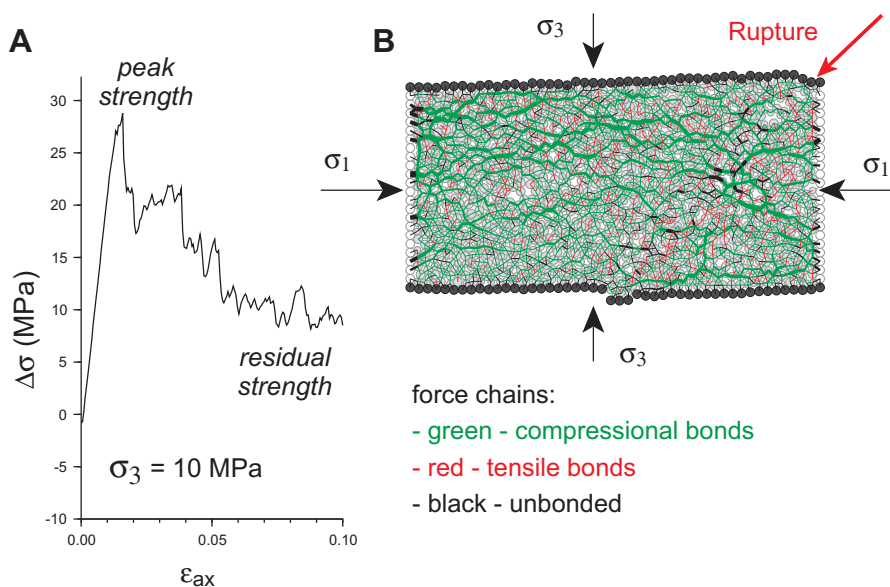


**Fig. 9.** Quantifying bulk mechanical properties for simulated particle dynamics materials. (A) Differential stress vs. strain plotted for a biaxial particle dynamics sample confined at 10 MPa, shows elastic loading to peak strength at failure, followed by irregular strain softening to residual strength associated with frictional sliding. (B) Snapshot of sample tested in (A), showing distribution of force chains which transmit stresses across the sample. The rupture zone is characterized by tensile bonds (red) and high compressional force unbonded contacts (black) that accommodate frictional sliding.

numerical modeling (e. g., Crook et al., 2006a, b; Albertz and Lingrey, 2012; Nolle et al., 2012). None of the above constitutive models accommodate anisotropic and/or rate-dependent (i.e. viscous, like salt) behavior that could be relevant for predicting in-situ stresses and deformation in some situations (Amadei, 1996; Day Lewis, 2007).

### 3.3. Damage mechanics

Damage mechanics is another powerful continuum-based constitutive formulation that is optimized to capture strain localization and softening behavior observed in brittle and quasi-brittle geologic materials. Damage mechanics models have been used extensively in fatigue analysis of metals, and to model evolution and progressive localization of deformation of rocks at the lab-scale (e.g., Buseti et al., 2012a; Gueguen and Besuelle, 2007; Ashby and Sammis, 1990). Damage mechanics has also recently been used to investigate problems such as the initiation of hydraulic fractures (Smart et al., 2012; Buseti et al., 2012b) and lithospheric scale deformation processes Karrech et al. (2011). To date, however, damage mechanics models have not seen significant use in modeling geologic structures at the scale of interest in this paper.

### 3.4. Constitutive properties for particle dynamics methods

Constitutive laws for particle dynamics simulations are not defined *a priori* in the same way as the continuum methods. Instead, the constitutive relationships depend on the assigned particle properties and interparticle interaction laws. However, the constitutive behaviors described above generally can be reproduced within particle assemblages using “soft-sphere” interparticle interactions. In fact, critical state, stress-dependent elasto-plastic behavior with hardening and strain softening responses are a natural outgrowth of the particulate nature of the model material. These behaviors reflect the changes in granular packing and dilatancy that accompany consolidation and shear (Mandl, 1988; Muir Wood, 1990; Marone et al., 1990).

A full specification of the constitutive behavior of simulated particle dynamics materials has not yet been carried out, although various characterization studies were conducted under specific loading paths, e.g., granular shear (Morgan, 1999, 2004), and Mohr–Coulomb failure criterion (e.g., Potyondy and Cundall, 2004; Dean et al., 2013), to address specific applications. As a demonstration, a biaxial test conducted on a confined cohesive particle assemblage (Fig. 9) exhibits elastic strain during initial axial loading, until reaching a peak strength, at which point discrete bonds begin to break, causing progressive strain softening until a through-going fracture develops. Similar simulations of this numerical material under different stress paths and loading conditions would more fully constrain the three-dimensional yield surface of such particle dynamics materials.

Given the large number of parameters that can influence the bulk behavior of the particle dynamics assemblages, model applications must focus on the effects of a few key parameters. The general objective of such modeling is to probe a range of parameter space to understand how these variables influence the final structural geometries and the mechanical evolution of the system. Such efforts provide valuable insights into how natural systems evolve, and the range of properties that may have existed at the time of deformation (Saltzer and Pollard, 1992; Morgan and Boettcher, 1999; Morgan, 1999; McGovern and Morgan, 2009).

One approach to overcome the lack of certainty about the constitutive response of discrete materials is referred to as SDEM (Egholm, 2007; Egholm et al., 2007). This strategy assigns constitutive properties in advance (i.e., Mohr–Coulomb parameters), and then fine-tunes the interparticle stresses to attain the desired continuum stresses. Such a hybrid approach offers more exact matching of desired constitutive properties, while retaining the ability for discontinuities to form and evolve that can arise in discrete systems. However, this approach is not appropriate for systems with complex, time-, space-, or stress-dependent constitutive behaviors, and loses some of the opportunities to gain insights into the micromechanics of deformation.

Commonly, the most internally consistent way to select appropriate particle and inter-particle properties for tectonic-scale

particle dynamics simulations is to match the characteristic geometries of the modeled systems with other observational data, e.g., of a small part of the system. In this way, particle properties can be iteratively modified until the right geometry is obtained. Nonetheless, the bulk constitutive properties for the chosen particle properties should be quantified and compared to predictions for natural materials. These tuned properties then can be used to simulate larger systems to examine regional stress conditions and tectonic evolution (Hardy et al., 2009; McGovern and Morgan, 2009).

#### 4. Numerical modeling considerations

##### 4.1. Model resolution

If the numerical tools and available constitutive laws suit the desired objective, one can set up one or more numerical modeling exercises. Several issues need to be addressed in preparation for such exercises. The first consideration for structural modeling is model resolution. A basic tenet of numerical modeling is that processes that are inherently discontinuous at a small scale can be modeled as a continuum when viewed at large enough scale (Munjiza, 2004). The difficulty for the modeler is determining which geological formations, properties and features can be safely combined or averaged and which must be specified explicitly in the model. Typically, this is achieved through trial and error (i.e., sensitivity studies) to determine if the included properties produce the expected behavior or geometries. Practically speaking, the elements or particles in these models need to be at least one-half to one-third the size of the features expected to be resolved. This constraint can result in a large number of calculations for each step in the model, leading to long run times. As noted above, run times scale nearly linearly with the number of elements or particles. Thus, halving the element or particle size for a given 2D domain size increases the number of calculations by a factor of  $\sim 4$ , quadrupling the CPU time required for a given time-step. For large and complex models, particularly in 3D, this can slow down run times to unacceptable levels, and highlights the inherent struggle between model resolution and run time.

##### 4.2. Discontinuities

The way faults and discontinuities are represented in these numerical models can also be an issue. Faults are narrow zones of intense shear deformation, which develop through a progressive change from distributed deformation to highly localized strain and associated softening (or strength deterioration) of the materials involved. Mechanically, they represent a strength discontinuity within the model, and the material properties of the rocks on either side of the fault may remain similar or may also be discontinuous. The first question for the modeler is whether to pre-define faults in the model, or to have them emerge when and where the conditions dictate. The answer to this question will almost dictate the type of modeling. Pre-defined faults are almost a necessity in continuum models, although pre-defined faults cannot be inserted in Arbitrary Lagrangian Eulerian-type continuum models. In contrast, the emergent behavior of discontinuities in particle dynamics facilitates modeling the conditions responsible for the onset of faulting. It is possible to pre-define zones of weakness or heterogeneity that localize faulting in particle dynamics models, although it is generally unnecessary to do so.

The process of fault initiation and strain localization in materials is described most completely by fracture mechanics theory, through the linkage of microscopic cracks and other heterogeneities (Reches and Lockner, 1994; Moore and Lockner, 1995). It is

generally impractical to track this process within the large domains of interest here. Fortunately, the initiation and orientation of faults is well predicted by elasto-plastic constitutive models based on the bulk material properties (Jaeger et al., 2007). However, the transition from a cohesive strength condition to frictional sliding on a newly formed fault is not well defined. The chosen rate of strength evolution will play a big role in how rapidly and completely strain localizes onto a modeled fault zone. This evolution is prescribed as part of the constitutive behavior for the continuum models, but emerges as a function of imposed particle and bond properties in the particle dynamics models, which must be tuned to obtain the desired result. A secondary concern is the demonstrated dependence of fault friction on slip velocity, maturity of contact, rock-mass stiffness, and temperature (e.g., Dieterich, 1972, 1979; Scholz, 1990; Marone et al., 1990; Beeler et al., 1996). However, most large-scale particle-based models avoid these issues by running in a quasi-static mode, using time-steps small enough to minimize the inertia of the system.

Many strategies also have been developed to modify or enhance the finite element method to capture discontinuities and intense shearing along faults or shear bands. These approaches include: (a) adaptive mesh refinement (e.g., Ortiz and Quigley, 1991; Crook et al., 2006a; Albertz and Sanz, 2012; Nollet et al., 2012), (b) the Arbitrary Lagrangian–Eulerian formulation (ALE) (e.g., Hirt et al., 1974; Fullsack, 1995; Wissing and Pfiffner, 2003; Stockmal et al., 2007; Ellis et al., 2004; Simpson, 2006; Ings and Beaumont, 2009), (c) contact mechanics (Laursen, 2002; Wriggers, 2002; Niño et al., 1998; Sanz et al., 2007, 2008; Griffith et al., 2009), (d) the embedded discontinuity approach (e.g., Regueiro and Borja, 1999; Borja et al., 2000), (e) the extended finite element method (e.g., Dolbow et al., 2001; Liu and Borja, 2009), and (f) the isogeometric finite element method (e.g., Benson et al., 2010; Verhoosel et al., 2010).

The most used techniques in structural geologic modeling are adaptive mesh refinement, the ALE approach, and contact mechanics. Techniques (a) and (b) are used to model the initiation and development of new faults, and (c) is used to capture the behavior of pre-existing faults and to better constrain boundary models. All of these approaches entail some form of regularization to characterize the thickness of the fault. Regularization is strategy to normalize fault zone thickness to element size, in order to minimize the effects of element size on the resulting pattern of deformation. In the contact mechanics approach, the thickness of the fault or sliding interface is assumed to be zero and therefore the displacement field is discontinuous across the slip surface. This approach has a disadvantage over (a) and (b) in that the fault geometry must be predefined and does not emerge naturally from the model. In the adaptive remeshing approach, the mesh is re-defined when elements become distorted beyond pre-set tolerances. The ALE approach uses two superimposed meshes. An Eulerian mesh remains fixed and orthogonal, and is relied upon for the calculations, while a second Lagrangian mesh is allowed to undergo quite extreme changes in shape.

##### 4.3. Boundary conditions and gravity loading

Finally, once the geometry of the model domain is designed, and the layers are populated with the appropriate mechanical properties, the modeler has to define the conditions that will drive deformation. Typically, prescribed boundary displacements are employed, forcing deformation into the rest of the domain (e.g., Albertz and Lingrey, 2012). The boundary may be considered an integral part of the domain, maintaining coherence and moving in tandem with the rest of the system. Alternatively, the boundary may approximate some far-field displacement field, in which case

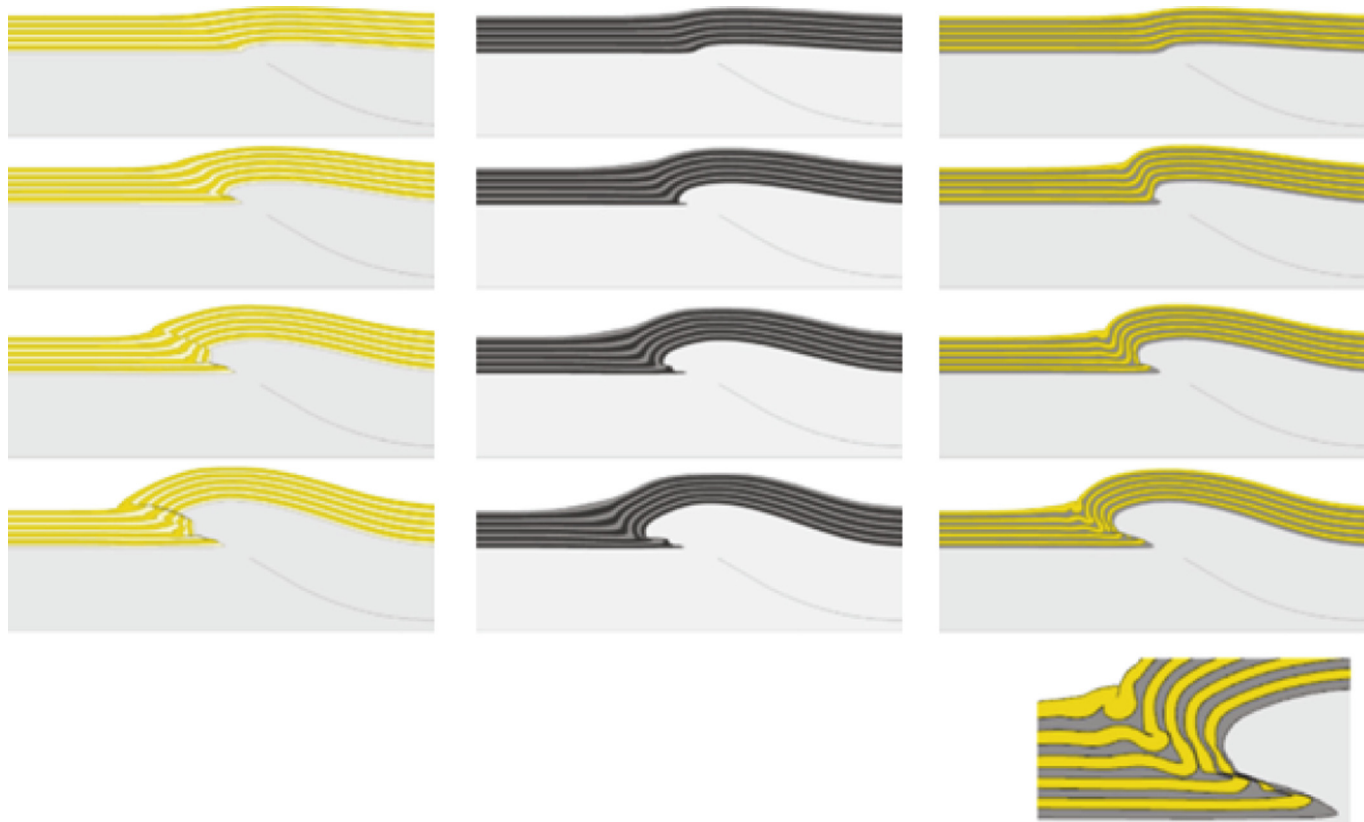


**Fig. 10.** An example of finite element models demonstrating the main capability of testing different sensitivities. In this example, the configuration and boundary conditions of the models were held constant, only the material model was varied. In sequence A, the colored layers are all normally-consolidated sandstone. In sequence B, all the colored layers are normally-consolidated shale. In sequence C, the yellow layers are sandstone, while the dark gray layers are shale. These types of models are very good at demonstrating changes in deformation style that accompany different starting conditions. It is difficult, however, to make models like this match specific examples observed in nature. Modified from [Albertz and Lingrey \(2012\)](#).

the model should be free to deform against the boundary, for example by introducing frictionless contact between the model materials and the boundary (e.g., [Sanz et al., 2008](#)). An alternative boundary condition relies on prescribed forces rather than displacements; however, given the tendency for modeled materials to undergo changes in strength during deformation, force-controlled boundary conditions tend to be less stable, and unpredictable. Gravity plays a significant role in the overall stress history of large geologic systems, and should be included, especially if absolute stress conditions during deformation are important. Gravity can be expressly included, or an effective gravity load can be imposed, depending upon how a model is set up. Scaling of the model can also be an issue in this regard. For example, a model constructed to mimic a scaled sandbox experiment may behave very differently when re-scaled to model a mountain belt or accretionary wedge.

## 5. Examples of finite element and particle dynamics models

A few representative examples of mechanical models are included here as demonstrations of what can be gained using these tools. The reader is guided to the many other published examples, cited here and elsewhere, to explore the broader range of opportunities ([Table 1](#))

Useful examples of the current state-of-the-art abilities of finite elements for structural modeling are presented in [Albertz and Sanz \(2012\)](#) and [Albertz and Lingrey \(2012\)](#) ([Fig. 10](#)). This is a parametric study of the interplay between mechanical stratigraphy (in particular the strength of the overburden) and fault geometries on resulting fold shapes in the deformed strata. The models were run

using the ELFEN software (Rockfield Software, Ltd., Swansea, Wales). The model domain is 10 km thick by 36 km wide. The upper 3 km represents a sedimentary overburden and the lower 7 km is crystalline basement.

These models utilize a critical state-type constitutive law for the material properties ([Crook et al., 2006a, b](#)). Many of the models presented employ a homogenous material, although strength increases with depth proportional to the weight of the overburden, and expressed as an over-consolidation ratio. Expressing strength as a ratio proportional to overburden is a convenient way to define the strength of the materials. The strength can be easily increased or decreased in subsequent model runs while preserving any existing inter-layer heterogeneity. It is also an efficient way to mimic the strengthening effects of diagenetic cementation.

The software in this example permits the insertion of sliding contact surfaces as pre-defined faults, and also features an adaptive remeshing capability to handle large strains within the mesh. The mesh is re-formed during any time-step in which a pre-specified strain limit is exceeded within any elements in the model. The refined mesh elements also grow smaller, again following pre-set limits. The net result is a controlled, progressive softening of regions undergoing high strain that in turn localizes the deformation. Thus, faults can terminate within the model, but a localized zone of deformation will propagate into the model as displacement occurs ([Fig. 11](#)). The structural features that emerge from these models are very geological in appearance.

A demonstration of the potential of particle dynamics simulations for the study of the kinematics and mechanics of tectonic-scale contractional deformation is shown in [Fig. 12](#). This example,

using the discrete element modeling code RICEBAL (Morgan and McGovern, 2005a; Dean et al., 2013) starts as a 120 km wide cohesive assemblage deformed by pushing the back wall inward above a weak decollement layer, located above the lower blue layer. Interparticle friction is set to 0.3 within the domain and is activated once the particle bonds break. By contrast, the decollement layer has no interparticle friction to facilitate sliding. The particle displacements and contact forces are recorded at every time-step throughout the simulation, so that equivalent continuum strains and stresses (or their invariants) can be calculated to analyze the behavior of the system.

Slip is localized along the weak decollement horizon, which drives deformation into the overlying domain. In this example, uniformly spaced forethrusts develop above the decollement, uplifting and folding the overlying strata to form a broadly tapered wedge. Substantial distributed lateral compaction precedes and accompanies thrusting, reflected in distributed blue domains in the right-hand panels (Fig. 12). When failure (faulting) occurs, it is accompanied by local dilation and strain softening, which favors frictional slip on the new fault. Local dilation of the uplifted strata also occurs as lateral confinement of thrust sheets decreases

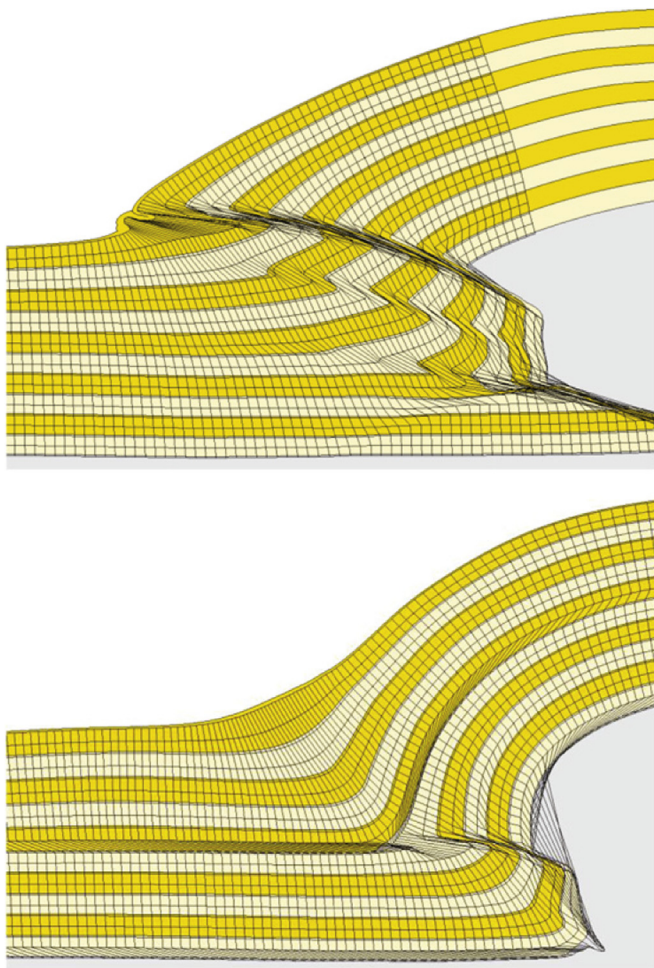


**Fig. 11.** Model detail showing localization of deformation within a model processed by the finite element code ELFEN™. The sharp offsets in the basement lithology, shown as gray material on lower right, are accommodated in the software by recomputing the mesh when distortion exceeds pre-set limits of internal strain. The thin, dark lines are a material grid that starts as a rectilinear grid and deforms as the experiment progresses. Modified from Albertz and Lingrey (2012).

(Fig. 12). These compactive, dilative, and critical-state phenomena demonstrate the ability of particle dynamics materials to reproduce many aspects of critical state mechanics.

As noted above, particle dynamics simulations also allow us to look into the mechanisms responsible for the observed deformation in fold and thrust belts, spanning the gap between discrete analog models and continuum finite element models, providing mechanical perspectives of discrete deformation processes that cannot be observed any other way. The stress evolution during deformation (and material stress paths if desired) can be mapped by gridding the directional components of the stress tensor at specific times during the simulation. Two scalar quantities, mean stress ( $\sigma_m = [\sigma_1 + \sigma_3]/2$ ), and differential stress ( $\Delta\sigma = \sigma_1 - \sigma_3$ ), and the orientation of the maximum compressive stress, ( $\sigma_1$ ) are derived and plotted to aid in the visualization of the stress tensor field. A third quantity, referred to as failure potential, denotes the proximity of the differential stress to the failure condition, and can be tracked during deformation.

As an example, Fig. 13 examines the initiation and propagation of a new thrust fault in front of an advancing thrust system. Initially, mean stress is highest close to the back wall and differential stress is greatest in the immediate footwall of the frontal thrust. This stress state results in a zone of high failure potential above the slipping decollement. As loading continues, a new thrust is formed in the high stress region, transferring the mean stress forward and releasing the differential stress above the newly formed fault. These changes, in turn, decrease the failure potential throughout the domain. The surrounding rocks return to an elastic loading path, i.e., within the critical state yield surface, accommodating slip on the new and pre-existing faults, until stress conditions in front of the new fault approach failure and the process begins anew.

## 6. Comparative forward modeling

Comparative numerical modeling plays a valuable role in forward modeling, particularly given the significant differences between various modeling approaches and assumptions, and the need for independent validation of numerical results. This realization was the motivation behind comparative benchmark modeling carried out by several different groups, using both continuum and particle dynamics approaches, as well as analog models (e.g., Ellis et al., 2004; Buiter et al., 2006). Both contractional and extensional systems were studied this way, with the models showing greater variability between codes for the contractional models. This type of comparative modeling effort serves to demonstrate the difficulties of exactly matching model material properties, as well as initial and boundary conditions, but can highlight the robust features that characterize the formation of thrust wedges (Buiter et al., 2006).

Finite element and particle dynamics simulations of the evolution of Sheep Mountain anticline, Bighorn basin, Wyoming have been compared by Zhang et al., (2013). Identical model domains, 27 km long and 3.45 km tall, were constructed for the two simulations. Nine stratigraphic layers with varying thicknesses and mechanical properties were placed over the basement. The positions and offsets of three basement faults were prescribed, and these were displaced into the overlying strata to form the structure. The final results for one set of basement displacements are shown in Fig. 14.

In both the finite element and particle dynamics model results, the sedimentary strata are passively deformed by predefined basement and side boundary displacements, which simulate the process of basement uplift and folding. Regional compression is applied by moving the right-hand wall to the left as the basement deforms. Deformation in both models is imposed in four stages,

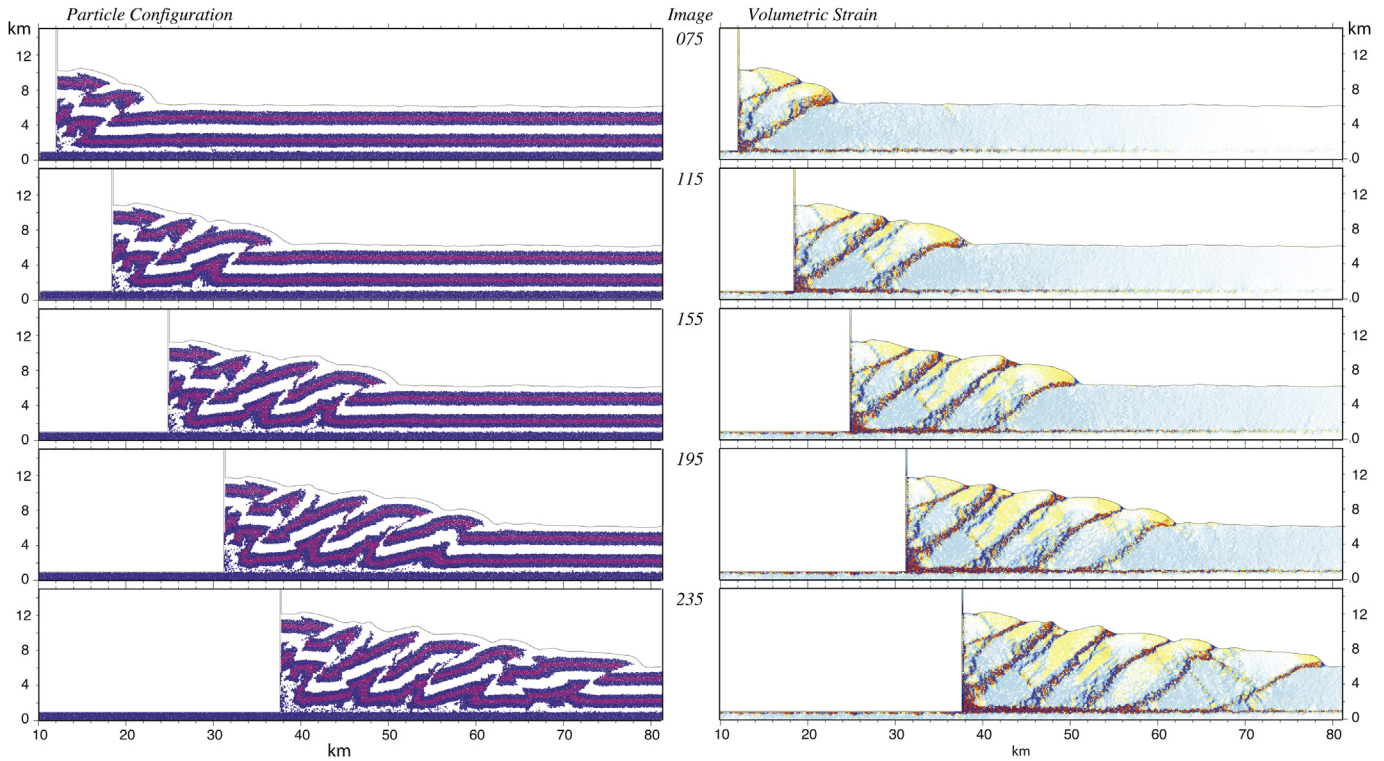


**Fig. 12.** Sequential snapshots of a contractional wedge simulation using the particle dynamics method, showing the development of evenly spaced imbricate thrust sheets in response to the inward displacement of the left wall. Left panels show the particle configuration for five displacement increments. The decollement layer lies immediately above the basal dark blue domain. The right panels show total volumetric strain (contraction is blue; dilation is red and yellow), demonstrating that distributed lateral compaction precedes and accompanies thrusting. Dilation of the rotated strata (yellow colors) also occurs as lateral confinement of thrust sheets decreases during uplift of the thrust slices.

similar to the hypothetical series of events proposed by Stanton and Erslev (2002). Each stage employs constant predefined basal displacement rates and corresponds to about 1 My, with resulting basement and boundary configurations shown in Fig. 14.

There is a close overall match between the finite element and particle dynamics results, although with some important differences. Overall, the thrust faults formed in the particle dynamics simulations are slightly steeper than in the finite element model, and

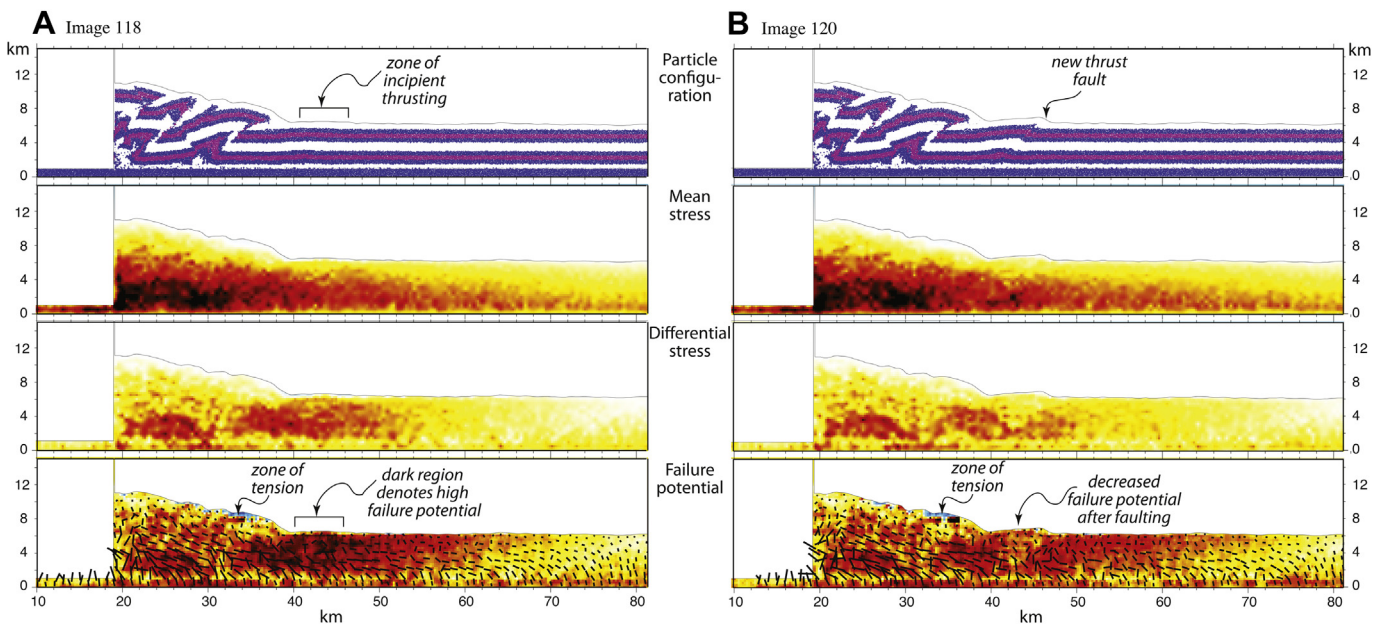


**Fig. 13.** Derived stress quantities for the contractional particle dynamics simulation shown in Fig. 12 during a thrust initiation sequence. In each stress plot, color intensity scales with stress magnitude. Top panel: particle configuration; second panel:  $\sigma_m$ ; third panel:  $\Delta\sigma$ ; bottom panel: failure potential with overlay of  $\sigma_1$  orientations (length scaled by  $\sigma_m$ ). (a) Image 118, pre-thrust: High  $\sigma_m$  occurs at depth within the wedge, close to the moving wall, and decreases to the right.  $\Delta\sigma$  is similarly high at depth beneath the wedge, but is also unusually high in footwall of frontal thrust. High failure potential occurs in the footwall where next thrust will form. Note blue stress potential on slope, reflecting tensile stresses. (b) Image 120, post-thrust: Propagation of the new forethrust within the footwall causes a decrease in  $\Delta\sigma$  and failure potential, although they remain high at depth where tectonic stress has been transferred forward above the decollement fault.

the particle dynamics model exhibits significantly more upper level extension and fracturing. This extension is accommodated through layer thinning in the finite element model. It appears that the differences between the two models relate partially to the different modes of deformation inherent to the type of model. The tensile fractures (discontinuities) observed in the particle dynamics models are more easily accommodated in discrete simulations, and also reflect the modeled high cohesive strengths in these shallow materials. Reducing the cohesive strengths tended to result in surficial flow of the shallower strata, inconsistent with the finite element results. The bed thinning observed in the finite element models is more typical of a continuum response for plastic materials. This discrepancy may reflect different modeled rheologies for these shallow materials. The differences in propagation rates of the various faults also imply fundamental differences in the constitutive behaviors of the two models. Strain rates are less easily controlled in particle dynamics simulations, compared to finite element models, where they are prescribed with the constitutive laws. In addition, the steeper faults in the particle dynamics models suggest that the bulk mechanical properties differ between the two models.

### 7. Comparison of geomechanical and geometric analysis techniques

For nearly the past thirty years, much structural interpretation has depended upon a purely geometrical ‘balancing’ approach that uses the core assumptions of conservation of cross-sectional area (i.e., volume) and bed length during deformation (Suppe, 1983; Suppe and Medwedeff, 1990, and many others). These assumptions allow the derivation of systematic geometric rules that can be

employed in cross section balancing analysis. While these types of approaches can be very efficient and informative, they neglect the mechanical aspects of rock deformation. For one, all rock types are assumed to obey the same geometric rules, with the exception of lithologies like salt and sometimes shale, which can experience significant flowage. For flowing materials, only constant area is required. This purely geometric approach leads to a variety of misfits between the geometric analyses and real-world structures (e.g. Cardozo et al., 2005). Some proposed modifications of the original rules have been put forward to deal with these misfits, including growth fault-bend folding (Medwedeff, 1989; Suppe et al., 1992), shear fault bend folding (Mosar and Suppe, 1992; Suppe et al., 2004) and tri-shear (Erslev, 1991; Hardy and Ford, 1997; Allmendinger, 1998) among others.

One specific source these misfits is the assumption of constant area (volume) during deformation, which is not a constraint in the earth, or for geomechanical models. A rock body can dilate, compact, or shear as a function of its mechanical state and past stress history. The mechanical properties in nature and in a numerical model can also vary from layer to layer. Mechanical forward models simultaneously satisfy the equilibrium differential equations, and the compatibility conditions for the kinematics, along with phenomenological stress–strain relations for the rock layers, so they are always in a mechanical ‘balance’. Careful geometric analyses of controlled mechanical modeling results needs to be carried out in the manner of Albrecht and Lingrey (2012) and Benesh et al. (2014) to assess the magnitude of errors that may arise from the geometric simplifications. This assessment is something that is now highly feasible, given the wealth of mechanical models of contractional systems.

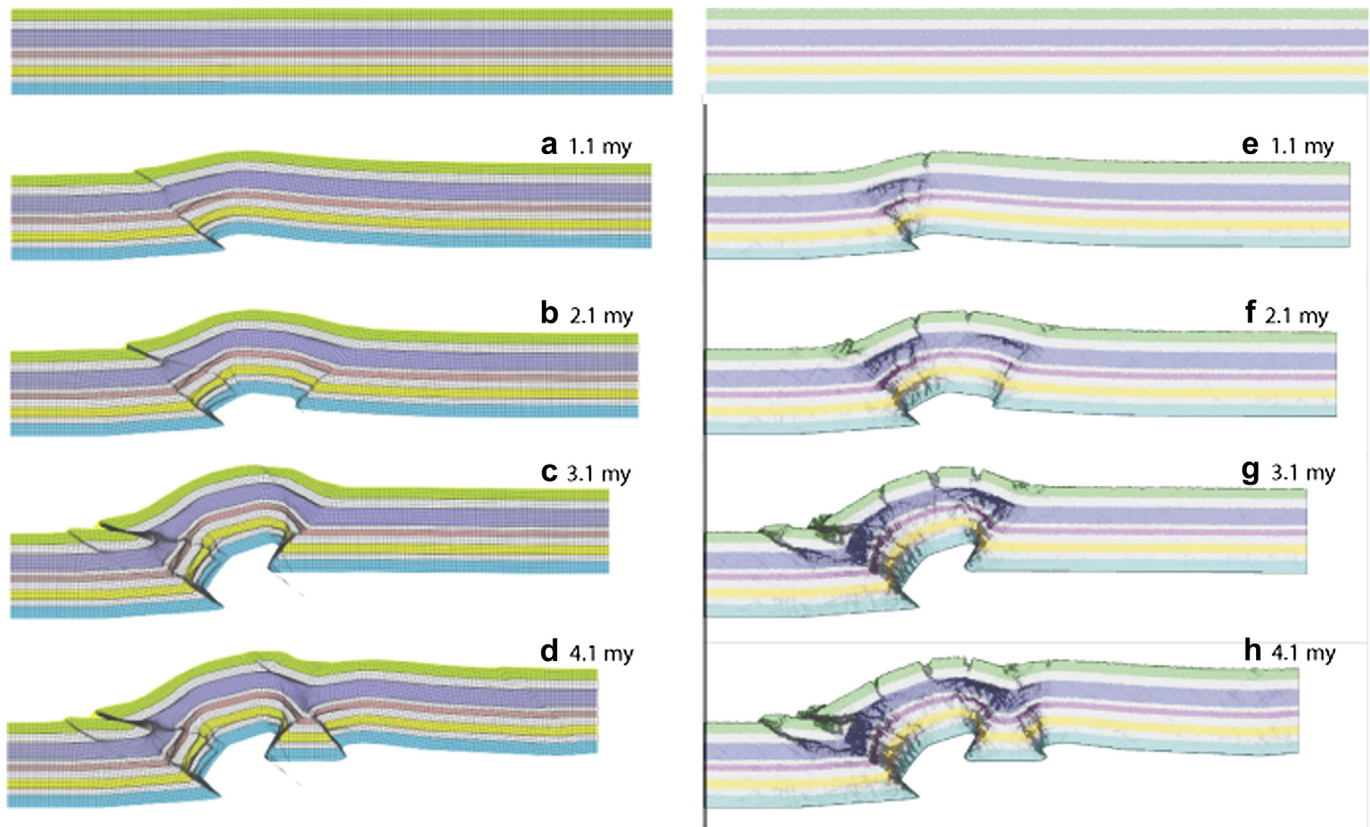


**Fig. 14.** Comparative modeling of evolution of Sheep Mountain, Bighorn Basin, Wyoming (after Zhang et al., 2013). Left panels: Sequential snapshots of finite element simulation at ~1 my increments. Offset and changes in layer thickness and distortion of the tracking mesh denote deformation. Right panels: Sequential snapshots of the discrete element simulation at the same stages of deformation. Superimposed gray shading shows regions of high distortion and shear strain.

A point of caution is appropriate here. Despite all the sophistication of forward mechanical modeling today, it is difficult and extremely time-consuming to create a forward model that precisely matches the geometry of a specific structure. Mechanical and geometric models serve very different purposes, and each has its own unique benefits. Geometric/kinematic models, especially the modified models, are adept at matching existing structures, drawing upon knowledge of many other known examples. This capability is especially important when trying to complete an interpretation on poorly-imaged seismic data. Forward mechanical models, with their sophisticated material descriptions, boundary conditions, emergent behavior, and predictive capabilities, provide key tests of the feasibility of these final interpretations, or constraints on the properties of the materials that compose them. In this way, the two techniques are highly complementary, and both have a place in the structural geologists' toolbox.

## 8. Conclusions

Several key ingredients are required for modeling the evolution of geologic structures. These ingredients include a solution method for non-linear models, a framework for capturing localized deformation or discontinuous displacement fields, a large-deformation formulation, appropriate constitutive laws that capture the salient features of rock behavior, and appropriate enhancements for capturing strain softening in continuum methods without mesh/particle size effects. These modeling techniques provide powerful tools to test and verify geologic interpretations or hypotheses that cannot be observed in nature or replicated in the lab due to the scale and nature of these phenomena.

The finite element method is by far the most common and useful of the continuum techniques. The integration scheme it employs makes it appropriate for the widest variety of geologic problems, and it can handle the most sophisticated constitutive relationships. Early problems with strain incompatibility are eased by several different strategies. The finite difference technique is the oldest of the continuum methods, but is less adaptable to many geologic problems. The boundary element method, due to its simple formulation and efficient meshing, can solve 3D problems with limited computational power.

Linear elasticity by itself is the least appropriate constitutive relationship commonly used in geologic models. There is no failure criterion, and it has a limited range of low-strain situations in which it is applicable. Traditional Mohr–Coulomb and Drucker–Prager plasticity models are a significant improvement over pure elasticity, but are inadequate if compactive yield behavior is important to the model results. Both laws have been modified to work in modern numerical simulation software, with Drucker–Prager being a more computationally friendly implementation. The most advanced constitutive relationships presented here are critical-state models. These can deal with significant complexities of behavior, including softening and hardening of the same material, dependent upon the stress paths experienced by the model.

Particle dynamics methods have also shown great applicability to modeling the formation of geologic structures. While the approach is different than finite elements, these techniques have inherently critical-state-like behavior by virtue of their particulate nature and the changes in granular packing that accompany shear and consolidation. It is very difficult to specifically define, however, the exact bulk stress–strain responses of the particle assemblages. These techniques provide a straightforward way to examine the mechanisms responsible for the observed deformation in contractional systems, and thus provide a unique window into the way thrust systems work.

The current state-of-the-art in numerical modeling offers some significant advances over geometric/kinematic modeling that takes little account of the materials that are deformed to create a structure. Mechanically based forward models simultaneously satisfy the equilibrium differential equations, the compatibility conditions for the kinematics, along with phenomenological stress–strain relations for rock behavior. Mechanical forward models are not a replacement for geometric/kinematic analysis, however. It is not possible to routinely create forward numerical models that will match the geometry and details of a specific structure, except in extremely simple cases. This limits the use of numerical models for every-day type structural interpretation problems. However, forward numerical models are well suited to probing some of the fundamental questions regarding how structures form and evolve, and in this role, are highly complementary to geometric models.

## Acknowledgments

The authors would like to thank Michelle Cooke, Kevin Smart, Bill Dunne, and Nora Dedontney for thorough reviews of this manuscript. Bill Symington, Ganesh Dasari, Rod Myers, Bashar Alramahi and Brian Crawford at ExxonMobil Upstream Research and Tony Crook and Dean Thornton at Rockfield Software are thanked for many spirited discussions regarding the ideas presented herein. ExxonMobil Upstream Research Co is also thanked for support of this work and for permission to publish these results. Morgan also received funding through NSF grant EAR-1145263.

## References

- ABAQUS 6.11 User Documentation, 2012. Internet Manual. Simulia. Retrieved 13 September.
- Abe, S., Mair, K., 2005. Grain fracture in 3D numerical simulations of granular shear. *Geophys. Res. Lett.* 32, L05305. <http://dx.doi.org/10.1029/2004GL022123>.
- Aharonov, E., Sparks, D., 2004. Stick-slip motion in simulated granular layers. *J. Geophys. Res.* 109, B09306. <http://dx.doi.org/10.1029/2003JB002597>.
- Albertz, M., Lingrey, S., 2012. Critical state finite element models of contractional fault-related folding: Part 1. Structural analysis. *Tectonophysics* 576–577, 133–149.
- Albertz, M., Sanz, P.F., 2012. Critical state finite element models of contractional fault-related folding: Part 2. Mechanical analysis. *Tectonophysics* 576–577, 150–170.
- Allen, M.P., Tildesley, D.J., 1987. *Computer Simulation of Liquids*. Oxford University Press, Oxford.
- Allmendinger, R.W., 1998. Inverse and forward numerical modeling of trishear fault-propagation folds. *Tectonics* 17, 640–656.
- Amadei, B., 1996. Importance of anisotropy when estimating and measuring in situ stresses in rock. *Int. J. Rock Mech. Mining Sci. Geomech. Abs.* 33, 293–325.
- Ashby, M.F., Sammis, C.G., 1990. The damage mechanics of brittle solids in compression. *Pure Appl. Geophys.* 133, 489–521.
- Atkinson, J.H., Bransby, P.L., 1978. *The Mechanics of Soils, an Introduction to Critical State Soil Mechanics*. McGraw-Hill, London.
- Barnichon, J.D., Charlier, R., 1996. Finite Element Modelling of the Competition between Shear Bands in the Early Stages of Thrusting: Strain Localization Analysis and Constitutive Law Influence. *Geological Society of London*, pp. 235–250. Special Publication 99.
- Bellahsen, N., Fiore, P.E., Pollard, D.D., 2006. From spatial variation of fracture patterns to fold kinematics: a geomechanical approach. *Geophys. Res. Lett.* 33, L02301 <http://dx.doi.org/10.1029/2005GL024189>.
- Beekman, F., Badi, M., van Wees, J.D., 2000. Faulting, fracturing and in situ stress prediction in the Ahnet Basin, Algeria – a finite element approach. *Tectonophysics* 320, 311–329.
- Beeler, N.M., Tullis, T.E., Weeks, J.D., 1996. Frictional behavior of large displacement experimental faults. *J. Geophys. Res.* 101, 8697–8715.
- Benesh, N.P., Plesch, A., Shaw, J.H., Frost, E.K., 2007. Investigation of growth fault bend folding using discrete element modeling: implications for signatures of active folding above blind thrust faults. *J. Geophys. Res.* 112, B03504. <http://dx.doi.org/10.1029/2006JB004466>.
- Benesh, N.P., Plesch, A., Shaw, J.H., 2014. Geometry, kinematics, and displacement characteristics of tear-fault systems: an example from the deep-water Niger Delta. *Am. Assoc. Pet. Geol. Bull.* 98. <http://dx.doi.org/10.1306/06251311013> (in press).
- Benson, D.J., Bazilevs, Y., Hsu, M.C., Hughes, T.J.R., 2010. Isogeometric shell analysis: the Reissner–Mindlin shell. *Comput. Methods Appl. Mech. Eng.* 199, 276–289.
- Bolton, M.D., 1986. The strength and dilatancy of sands. *Geotechnique* 36, 65–78.

- Borja, R.I., Regueiro, R.A., Lai, T.Y., 2000. FE modeling of strain localization in soft rock. *J. Geotech. Geoenviron. Eng.* 126, 335–343.
- Braun, J., Sambridge, M., 1994. Dynamical Lagrangian Remeshing (DLR): a new algorithm for solving large strain deformation problems and its application to fault-propagation folding. *Earth Planet. Sci. Lett.* 124, 211–220.
- Brebbia, C.A., Dominguez, J., 1989. *Boundary Elements, an Introductory Course*. McGraw-Hill College.
- Buiter, S.J.H., Babeyko, A.Y., Ellis, S., Gerya, T., Kaus, B.J.P., Kellner, A., Schreurs, G., Yamada, Y., 2006. The numerical sandbox: comparison of model results for a shortening and an extension experiment. In: Buiter, S.J.H., Schreurs, G. (Eds.), *Analogue and Numerical Modelling of Crustal-scale Processes*. Geological Society, London, pp. 29–54. Special Publication 253.
- Burbridge, D.R., Braun, J., 2002. Numerical models of the evolution of accretionary wedges and fold-and-thrust belts using the distinct element method. *Geophys. J. Int.* 148, 542–561.
- Busetti, S., Mish, K., Reches, Z., 2012a. Damage and plastic deformation of reservoir rocks: Part 1. Damage fracturing. *Am. Assoc. Pet. Geol. Bull.* 96, 1687–1709.
- Busetti, S., Mish, K., Hennings, P., Reches, Z., 2012b. Damage and plastic deformation of reservoir rocks: Part 2. Propagation of a hydraulic fracture. *Am. Assoc. Pet. Geol. Bull.* 96, 1711–1732.
- Cardozo, N., Bawa-Bhalla, K., Zehnder, A., Allmendinger, R.W., 2003. Mechanical models of fault propagation folds and comparison to the trishear kinematic model. *J. Struct. Geol.* 25, 1–18.
- Cardozo, N., Allmendinger, R.W., Morgan, J.K., 2005. Influence of mechanical stratigraphy and initial stress state on the formation of two fault propagation folds. *J. Struct. Geol.* 27, 1954–1972.
- Chen, W.F., 1982. *Plasticity in Reinforced Concrete*. McGraw-Hill, New York, pp. 190–252.
- Colmenares, L.B., Zoback, M.D., 2002. A statistical evaluation of intact rock failure criteria constrained by polyaxial test data for five different rocks. *Int. J. Rock Mech. Mining Sci.* 39, 695–729.
- Cooke, M.L., Pollard, D.D., 1997. Bedding-plane slip in initial stages of fault-related folding. *J. Struct. Geol.* 19, 567–581.
- Cooke, M.L., Mollema, P., Pollard, D.D., Aydin, A., 2000. Interlayer slip and joint localization in East Kaibab Monocline, Utah: field evidence and results from numerical modeling. In: Cosgrove, J.W., Ameen, M.S. (Eds.), *Forced Folds and Fractures*, Geological Society Special Publication 169, pp. 23–49.
- Cooke, M.L., Underwood, C.A., 2001. Fracture termination and step-over at bedding interfaces due to frictional slip and interface opening. *J. Struct. Geol.* 23, 223–238.
- Coulomb, C.A., 1773. Sur l'application des règles de maxima et minima à quelques problèmes de statique relatifs à l'Architecture (Application of the rules of maxima and minima to some problems of statics related to architecture). *Mémoires de Mathématique et de Physique, Académie Royale des Sciences* 7, 343–382.
- Couples, G.D., Lewis, H., Olden, P., Workman, G.H., Higgs, N.G., 2007. Insights into the faulting process from numerical simulations of rock-layer bending. *Geol. Soc. London Spec. Pub.* 289, 161–186 <http://dx.doi.org/10.1144/SP289.10>.
- Crook, A.J.L., Owen, D.R.J., Willson, S.M., Yu, J.G., 2006a. Benchmarks for the evolution of shear localisation with large relative sliding in frictional materials. *Comput. Methods Appl. Mech. Eng.* 195, 4991–5010.
- Crook, A.J.L., Willson, S.M., Yu, J.G., Owen, D.R.J., 2006b. Predictive modelling of structure evolution in sandbox experiments. *J. Struct. Geol.* 28, 729–744.
- Cundall, P.A., 1971. A computer model for simulating progressive large scale movements in blocky rock systems. In: *Proceedings of the Symposium of International Society of Rock Mechanics 1*, Nancy, France, Paper II-8.
- Cundall, P.A., Strack, O.D.L., 1979. A discrete numerical model for granular assemblies. *Geotechnique* 29, 47–65.
- Cundall, P.A., Strack, O.D.L., 1983. Modeling of microscopic mechanisms in granular materials. In: Jenkins, J.T., Satake, M. (Eds.), *Mechanics of Granular Materials: New Models and Constitutive Relations*. Elsevier Science, New York, pp. 137–149.
- Day-Lewis, A.D.F., 2007. *Characterization and Modeling of In Situ Stress Heterogeneity*. Ph.D. thesis. Stanford Univ., Stanford, Calif.
- Dean, S.L., Morgan, J.K., Fournier, T., 2013. Geometries of frontal fold and thrust belts: insights from discrete element simulations. *J. Struct. Geol.* 53, 43–53.
- Detournay, C., Hart, R., 1999. FLAC and numerical modelling in geomechanics. In: *Proceedings of the International FLAC Symposium on Numerical Modelling in Geomechanics*, Minneapolis. Balkema, Rotterdam.
- Dieterich, J.H., 1972. Time dependent friction in rocks. *J. Geophys. Res.* 77, 3690–3697.
- Dieterich, J.H., 1979. Modeling of rock friction: 1. Experimental results and constitutive equations. *J. Geophys. Res.* 84, 2161–2168.
- Dolbow, J., Moës, N., Belytschko, T., 2001. An extended finite element method for modeling crack growth with frictional contact. *Comput. Methods Appl. Mech. Eng.* 190, 6825–6846.
- Drucker, D.C., Prager, W., 1952. Soil mechanics and plastic analysis for limit design. *Quart. Appl. Math.* 10, 157–165.
- Drucker, D.C., Gibson, R.E., Henkel, D.J., 1957. Soil mechanics and work-hardening theories of plasticity. *Transact. Am. Soc. Civil Eng.* 122, 338–346.
- Durand-Riard, P., Shaw, J.H., Plesch, A., Lufadeju, G., 2013. Enabling 3D geomechanical restoration of strike- and oblique-slip faults using geological constraints, with applications to the deep-water Niger Delta. *J. Struct. Geol.* 48, 33–44.
- Egholm, D.L., 2007. A new strategy for discrete element numerical models: 1. Theory. *J. Geophys. Res.* 112, B05203. <http://dx.doi.org/10.1029/2006JB004557>.
- Egholm, D.L., Sandiford, M., Clausen, O.R., Nielsen, S.B., 2007. A new strategy for discrete element numerical models: 2. Sandbox applications. *J. Geophys. Res.* 112, B05204. <http://dx.doi.org/10.1029/2006JB004558>.
- Egholm, D.L., Clausen, O.R., Sandiford, M., Kristensen, M.B., Korstgård, J.A., 2008. The mechanics of clay smearing along faults. *Geology* 36, 787–790. <http://dx.doi.org/10.1130/G24975A.1>.
- Ellis, S., Schreurs, G., Panien, M., 2004. Comparisons between analogue and numerical models of thrust wedge development. *J. Struct. Geol.* 26, 1675–1695.
- Erickson, S.G., 1993. Sedimentary loading, lithospheric flexure, and subduction initiation at passive margins. *Geology* 21, 125–128.
- Erickson, S.G., Jamison, W.R., 1995. Viscous-plastic finite-element models of fault-bend folds. *J. Struct. Geol.* 17, 561–573.
- Erickson, S.G., Strayer, L.M., Suppe, J., 2004. Numerical modeling of hinge-zone migration in fault-bend folds. In: K. R. McClay, ed., *Thrust Tectonics and Hydrocarbon Systems*. Am. Assoc. Pet. Geol. Mem. 82, 438–452.
- Erickson, S.G., Strayer, L.M., Suppe, J., 2001. Initiation and reactivation of faults during movement over a thrust-fault ramp: numerical mechanical models. *J. Struct. Geol.* 23, 11–23.
- Erickson, S.G., 1995. Mechanics of triangle zones and passive-roof duplexes: implications of finite-element models. *Tectonophysics* 245, 1–11.
- Erslev, E.A., 1991. Trishear fault-propagation folding. *Geology* 19, 617–620.
- Finch, E., Hardy, S., Gawthorpe, R., 2004. Discrete-element modelling of extensional fault-propagation folding above rigid basement fault blocks. *Basin Res.* 16, 467–488.
- Fiore, P.E., Pollard, D.D., Currin, W., Miner, D.M., 2007. Mechanical and stratigraphic constraints on the evolution of faulting at Elk Hills, CA. *Am. Assoc. Pet. Geol. Bull.* 91, 321–341.
- Fullsack, P., 1995. An arbitrary Lagrangian–Eulerian formulation for creeping flows and its application in tectonic models. *Geophys. J. Int.* 120, 1–23.
- Gerbault, M., Poliakov, A.N.B., Daignieres, M., 1998. Prediction of faulting from the theories of elasticity and plasticity, what are the limits? *J. Struct. Geol.* 20, 301–320.
- Georgiannopoulos, N.G., Brown, E.G., 1978. The critical state concept applied to rock. *Int. J. Rock Mech. Min. Sci. Geomech. Abs.* 15, 1–10.
- Gerya, T., 2010. *Introduction to Numerical Geodynamic Modelling*. Cambridge University Press, ISBN 9780521887540.
- González, G., Gerbault, M., Martinod, J., Cembrano, J., Carrizo, D., Allmendinger, R., Espina, J., 2008. Crack formation on top of propagating reverse faults of the Chuculay Fault System, northern Chile: insights from field data and numerical modeling. *J. Struct. Geol.* 30, 791–808.
- Goodman, R.E., 1989. *Introduction to Rock Mechanics*, second ed. John Wiley & Sons.
- Griffith, A.A., 1921. The phenomena of rupture and flow in solids. *Phil. Tran. Roy. Soc. London, Ser. A* 221, 163–198.
- Griffith, W.A., Sanz, P.F., Pollard, D.D., 2009. Influence of outcrop scale fractures on the effective stiffness of fault damage zone rocks. *Pure Appl. Geophys.* 166, 1595–1627. <http://dx.doi.org/10.1007/s00024-009-0519-9>.
- Guiton, M.L.E., Sassi, W., Bertrand, Y.M., Gauthier, D.M., 2003b. Mechanical constraints on the chronology of fracture activation in folded Devonian sandstone of the western Moroccan Anti-Atlas. *J. Struct. Geol.* 25, 1317–1330.
- Gueguen, Y., Besuelle, P., 2007. *Damage and Localization: two Key Concepts in Rock Deformation Studies*. Geological Society London, pp. 7–17. <http://dx.doi.org/10.1144/SP289.2>. Special Publications 289.
- Guiton, M., Leroy, Y., Sassi, W., 2003a. Activation of diffuse discontinuities and folding of the sedimentary layers. *J. Geophys. Res.* 108, 2183.
- Guo, Y., Morgan, J.K., 2006. The frictional and micromechanical effects of grain comminution in fault gouge from distinct element simulations. *J. Geophys. Res.* 111, B12406. <http://dx.doi.org/10.1029/2005JB004049>.
- Guo, Y., Morgan, J.K., 2007. Fault gouge evolution and its dependence on normal stress and rock strength – results of discrete element simulations: gouge zone properties. *J. Geophys. Res.* 112, B10403. <http://dx.doi.org/10.1029/2006JB004524>.
- Guzowski, C., Mueller, J.P., Shaw, J.H., Muron, P., Medwedeff, D.A., Bilotti, F., Rivero, C., 2009. Insights into the mechanisms of fault-related folding provided by volumetric structural restorations using spatially varying mechanical constraints. *Am. Assoc. Pet. Geol. Bull.* 93, 1427–1446.
- Hardy, S., 2008. Structural evolution of calderas: insights from two-dimensional discrete element simulations. *Geology* 36, 927–930. <http://dx.doi.org/10.1130/G25133A.1>.
- Hardy, S., Ford, M., 1997. Numerical modeling of trishear fault propagation folding. *Tectonics* 16, 841–854.
- Hardy, S., McClay, K., Muñoz, J.A., 2009. Deformation and fault activity in space and time in high-resolution numerical models of doubly vergent thrust wedges. *Mar. Petrol. Geol.* 26, 232–248.
- Harrison, J.P., Hudson, J.A., 2000. *Engineering Rock Mechanics, Part 2: Illustrative Workable Examples*. Pergamon, Oxford.
- Hart, R., Cundall, P.A., Lemos, J., 1988. Formulation of a three dimensional distinct element model—part II. Mechanical calculations for motion and interaction of a system composed of many polyhedral blocks. *Int. J. Rock Mech. Mining Sci. Geomech. Abs.* 25, 117–125.
- Henk, A., 2006. A numerical sandbox: high-resolution distinct element models of half-graben formation. *Int. J. Earth Sci.* 95, 189–203.
- Hill, R., 1950. *The Mathematical Theory of Plasticity*. Oxford University Press, London.

- Hilley, G.E., Mynatt, I., Pollard, D.D., 2010. Structural geometry of Raplee Ridge monocline and thrust fault imaged using inverse boundary element modeling and ALSM data. *J. Struct. Geol.* 32, 45–58.
- Hirt, C.W., Amsden, A.A., Cook, J.L., 1974. An arbitrary Lagrangian Eulerian computing method for all speeds. *J. Com. Physiol.* 14, 227–253.
- Ings, S.J., Beaumont, C., 2009. Continental margin shale tectonics: preliminary results from coupled fluid-mechanical models of large-scale delta instability. In: Healy, D., Butler, R.W.H., Shipton, Z.K., Sibson, R.H. (Eds.), *Faulting, Fracturing and Igneous Intrusion in the Earth's Crust*. Geological Society London, pp. 571–582. Special Publication 367.
- Jaeger, J., Cook, N.G., Zimmerman, R., 2007. *Fundamentals of Rock Mechanics*, fourth ed. Blackwell, Malden, MA.
- Jamison, W.R., 1996. Mechanical models of triangle zone evolution. *Bull. Can. Pet. Geol.* 44, 180–194.
- Jones, M., 1994. Mechanical principles of sediment deformation. In: Maltman, A. (Ed.), *Geological Deformation of Sediments*. Chapman and Hall, London, pp. 37–72.
- Jones, M.E., Addis, M.J., 1986. The application of stress path and critical state analysis to sediment deformation. *J. Struct. Geol.* 8, 575–580.
- Karig, D.E., Morgan, J.K., 1994. Stress paths and strain histories during tectonic deformation of sediments. In: Maltman, A. (Ed.), *Geological Deformation of Sediments*. Chapman and Hall, London, pp. 167–204.
- Karrech, A., Regenauer-Lieb, K., Poulet, T., 2011. Continuum damage mechanics for the lithosphere. *J. Geophys. Res.* 16 (B4). <http://dx.doi.org/10.1029/2010JB007501>.
- Kwon, S., Mitra, G., 2004. Three-dimensional kinematic history at an oblique ramp, Leamington zone, Sevier belt, Utah. *J. Struct. Geol.* 8, 474–493.
- Laursen, T.A., 2002. *Computational Contact and Impact Mechanics: Fundamentals of Modelling Interfacial Phenomena in Nonlinear Finite Element Analysis*. Springer, Berlin.
- Laursen, T.A., Simo, J.C., 1993. Algorithmic symmetrization of coulomb frictional problems using augmented Lagrangians. *Comput. Methods Appl. Mech. Eng.* 108, 133–146.
- Li, S., Liu, W.K., 2004. *Mesh-free Particle Methods*. Springer, New York.
- Lin, X., Ng, T.T., 1997. A three-dimensional discrete element model using arrays of ellipsoids. *Geotechnique* 47, 319–329.
- Liu, F., Borja, R.I., 2009. An extended finite element framework for slow-rate frictional faulting with bulk plasticity and variable friction. *Int. J. Numer. Anal. Methods Geomech.* 33, 1535–1560.
- Maerten, L., Maerten, F., 2006. Chronologic modeling of faulted and fractured reservoirs using geomechanically based restoration: technique and industry applications. *Am. Assoc. Pet. Geol. Bull.* 90, 1201–1226.
- Maerten, L., Willemsse, M.J., Pollard, D.D., Rawnsley, K., 1999. Slip distributions on intersecting normal faults. *J. Struct. Geol.* 21, 259–271.
- Maerten, L., Gillespie, P., Daniel, J., 2006. Three-dimensional geomechanical modeling for constraint of subseismic fault simulation. *Am. Assoc. Pet. Geol. Bull.* 90, 1337–1358.
- Maerten, L., Gillespie, P., Pollard, D.D., 2002. Effects of local stress perturbation on secondary fault development. *J. Struct. Geol.* 24, 145–153.
- Mäkel, G., Walters, J., 1993. Finite-element analysis of thrust tectonics: computer simulation of detachment phase and development of thrust faults. *Tectonophysics* 226, 167–185.
- Maniatis, G., Hampel, H., 2008. Along-strike variations of the slip direction on normal faults: insights from three-dimensional finite-element models. *J. Struct. Geol.* 30, 21–28.
- Mandl, G., 1988. *Mechanics of Tectonic Faulting*. Elsevier Sci., New York.
- Mandl, G., 1990. Modelling incipient tectonic faulting in the brittle crust of the earth. In: Rossmanith, H.P. (Ed.), *Mechanics of Jointed and Faulted Rock*. Balkema, Rotterdam, pp. 29–40.
- Marone, C., Raleigh, C.B., Scholz, C.H., 1990. Frictional behavior and constitutive modeling of simulated fault gouge. *J. Geophys. Res.* 95, 7007–7025.
- McGovern, P.J., Morgan, J.K., 2009. Volcanic spreading and lateral variations in the structure of Olympus Mons, Mars. *Geology* 37, 139–142. <http://dx.doi.org/10.1130/G25180A.1>.
- Medwedeff, D.A., 1989. Growth fault-bend folding at southeast Lost Hills, San Joaquin valley, California. *Am. Assoc. Pet. Geol. Bull.* 73, 54–67.
- Melosh, H.J., Williams, C.A., 1989. Mechanics of graben formation in crustal rocks: a finite element analysis. *J. Geophys. Res.* 94, 13,961–13,973.
- Miyakawa, A., Y., Matsuoka, T., 2010. Effect of increased shear stress along a plate boundary fault on the formation of an out-of-sequence thrust and a break in surface slope within an accretionary wedge, based on numerical simulations. *Tectonophysics* 484, 127–138.
- Mogi, K., 1967. Effect of the intermediate principal stress on rock failure. *J. Geophys. Res.* 72, 5117–5131.
- Mohapatra, G.K., Johnson, R.A., 1998. Localization of listric faults at thrust ramps beneath the Great Salt Lake Basin, Utah: evidence from seismic imaging and finite element modeling. *J. Geophys. Res.* 103, 10,047–10,063. <http://dx.doi.org/10.1029/98JB00023>.
- Mohr, O., 1900. Welche Umstände bedingen die Elastizitätsgrenze und den Bruch eines Materials? (What are the conditions for the elastic limit and the fracturing of a material?) *Z. Ver. dt. Ing.* 44, 1524–1530, 1572–1577.
- Mohr, O., 1914. *Abhandlungen aus dem Gebiete der Technische Mechanik (Treatise on Topics in Engineering Mechanics)*, second ed. Ernst und Sohn, Berlin.
- Moore, D.E., Lockner, D.A., 1995. The role of microcracking in shear-fracture propagation in granite. *J. Struct. Geol.* 17, 95–114.
- Mora, P., Place, D., 1993. A lattice solid model for the non-linear dynamics of earthquakes. *Int. J. Modern Phys. C* 4, 1059–1074.
- Morgan, J.K., 1999. Numerical simulations of granular shear zones using the distinct element method: II. The effect of particle size distribution and interparticle friction on mechanical behavior. *J. Geophys. Res.* B 104, 2721–2732.
- Morgan, J.K., 2004. Particle dynamics simulations of rate and state dependent frictional sliding of granular fault gouge. *Pure Appl. Geophys.* 161, 1877–1891.
- Morgan, J.K., Boettcher, M.S., 1999. Numerical simulations of granular shear zones using the distinct element method: I. Shear zone kinematics and micro-mechanics of localization. *J. Geophys. Res.* B 104, 2703–2719.
- Morgan, J.K., McGovern, P.J., 2005a. Discrete element simulations of gravitational volcanic deformation: 1. Deformation structures and geometries. *J. Geophys. Res.* 110, B05402. <http://dx.doi.org/10.1029/2004JB003252>.
- Morgan, J.K., McGovern, P.J., 2005b. Discrete element simulations of gravitational volcanic deformation: 2. Mechanical analysis. *J. Geophys. Res.* 110, B05403. <http://dx.doi.org/10.1029/2004JB003253>.
- Morris, A.P., Ferrill, D.A., 2009. The importance of the effective intermediate principal stress ( $\sigma_2$ ) to fault slip pattern. *J. Struct. Geol.* 31, 950–959.
- Mosar, J., Suppe, J., 1992. Role of shear in fault-propagation folding. In: McClay, K.R. (Ed.), *Thrust Tectonics*. Chapman and Hall, London, pp. 123–132.
- Muir Wood, D., 1990. *Soil Behavior and Critical State Soil Mechanics*. Cambridge University Press, New York.
- Munjiza, A.A., 2004. *The Combined Finite-discrete Element Method*. Wiley and Sons, London.
- Naylor, M., Sinclair, H.D., Willett, S., Cowie, P.A., 2005. A discrete element model for orogenesis and accretionary wedge growth. *J. Geophys. Res.* 110, B12404. <http://dx.doi.org/10.1029/2003JB002940>.
- Niño, F., Philip, H., Chéry, J., 1998. The role of bed-parallel slip in the formation of blind thrust faults. *J. Struct. Geol.* 20, 503–516.
- Nollet, S., Kleine Vennekate, G.J., Giese, S., Vrolijk, P., Urai, J.L., Ziegler, M., 2012. Localization patterns in sandbox-scale numerical experiments above a normal fault in basement. *J. Struct. Geol.* 39, 199–209.
- Oda, M., Iwashita, K. (Eds.), 1999. *Mechanics of Granular Materials: an Introduction*. A.A. Balkema, Rotterdam.
- Ortiz, M., Quigley IV, J.J., 1991. Adaptive mesh refinement in strain localization problems. *Comput. Methods Appl. Mech. Eng.* 90, 781–804.
- Panjan, J., Wiltschko, D., 2004. Ramp initiation in a thrust wedge. *Nature* 427, 624–627.
- Parry, R.H., 2004. *Mohr Circles, Stress Paths, and Geotechnics*. Spon Press, London.
- PFC, 1999. *User's Guide Version 3.0*. Itasca Consulting Group, Inc.
- Place, D., Mora, P., 1999. The lattice solid model to simulate the physics of rocks and earthquakes: incorporation of friction. *J. Com. Physiol.* 150, 332–372.
- Plimpton, S.J., 1995. Fast parallel algorithms for short-range molecular dynamics. *J. Comp. Physiol.* 117, 1–19.
- Plimpton, S.J., Hendrickson, B.A., 1996. A new parallel method for molecular-dynamics simulation of macromolecular systems. *J. Comput. Chem.* 17, 326–337.
- Poliakov, A.N.B., Podladchikov, Y., Talbot, C., 1993. Initiation of salt diapirs with frictional overburdens: numerical experiments. *Tectonophysics* 228, 199–210.
- Potts, D.M., Zdravkovic, L., 1999. *Finite Element Analysis in Geotechnical Engineering*. Thomas Telford Ltd., London.
- Potyondy, D.O., Cundall, P.A., 2004. A bonded-particle model for rock. *Int. J. Rock Mech. Mining Sci.* 41, 1329–1364.
- Radjai, F., Dubois, F., 2011. *Discrete-element Modeling of Granular Materials*. Wiley-Iste.
- Reches, Z., Lockner, D., 1994. Nucleation and growth of faults in brittle rocks. *J. Geophys. Res.* 99, 18,159–18,173.
- Regueiro, R.A., Borja, R.I., 1999. Plane strain finite element analysis of pressure sensitive plasticity with strong discontinuity. *Int. J. Solids Struct.* 38, 3647–3672.
- Resor, P.G., Flodin, E.A., 2010. Forward modeling syndimentary deformation associated with a prograding steep-sloped carbonate margin. *J. Struct. Geol.* 32, 170–183.
- Resor, P.G., Pollard, D.D., 2012. Reverse drag revisited: why footwall deformation may be the key to inferring listric fault geometry. *J. Struct. Geol.* 41, 98–109.
- Roscoe, K.H., Schofield, A.N., Wroth, C.P., 1958. On the yielding of soils. *Geotechnique* 8, 22–53. London.
- Rothenburg, L., Bathurst, R.J., 1992. Micromechanical features of granular assemblies with planar elliptical particles. *Geotechnique* 39, 601–614.
- Saltzer, S.D., Pollard, D.D., 1992. Distinct element modeling of structures formed in sedimentary overburden by extensional reactivation of basement normal faults. *Tectonics* 11, 165–174.
- Sanz, P.F., 2008. *Modeling Rock Folding with Large Deformation Frictional Contact Mechanics*. Ph.D. thesis. Stanford University, California, USA.
- Sanz, P.F., Borja, R.I., Pollard, D.D., 2007. Mechanical aspects of thrust faulting driven by far-field compression and their implications to fold geometry. *Acta Geotechnica* 2, 17–31.
- Sassi, W., Faure, J.-L., 1997. Role of faults and layer interfaces on the spatial variation of stress regimes in basins: inferences from numerical modelling. *Tectonophysics* 266, 101–119.
- Sanz, P.F., Pollard, D.D., Allwardt, P., Borja, R.I., 2008. Mechanical models of fracture reactivation and slip on bedding surfaces during folding of the asymmetric anticline at sheep mountain, Wyoming. *J. Struct. Geol.* 30, 1177–1191.

- Savage, H.M., Cooke, M.L., 2003. Can flat-ramp-flat fault geometry be inferred from fold shape?: a comparison of kinematic and mechanical folds. *J. Struct. Geol.* 25, 2023–2034.
- Savage, H.M., Cooke, M.L., 2004. The effect of non-parallel thrust fault interaction on fold patterns. *J. Struct. Geol.* 26, 909–917.
- Schofield, A.N., Wroth, C.P., 1968. *Critical State Soil Mechanics*. McGraw-Hill, London, England.
- Scholz, C.H., 1990. *The Mechanics of Earthquakes and Faulting*. Cambridge University Press, New York.
- Schultz-Ela, D.D., 2002. Origin of drag folds bordering salt diapirs. *Am. Assoc. Pet. Geol. Bull.* 87, 757–780.
- Shamir, G., Eyal, Y., 1995. Elastic modeling of fault-driven monoclinical fold patterns. *Tectonophysics* 245, 13–24.
- Sheldon, H.A., Barnicoat, A.C., Ord, A., 2006. Numerical modelling of faulting and fluid flow in porous rocks: an approach on critical state soil mechanics. *J. Struct. Geol.* 28, 1468–1482.
- Simpson, G.D.H., 2006. Modelling interactions between fold-thrust belt deformation, foreland flexure and surface mass transport. *Basin Res.* 18, 125–143.
- Simpson, G., 2011. Mechanics of non-critical fold-thrust belts based on finite element models. *Tectonophysics* 499, 142–155.
- Simpson, G.D.H., 2009. Mechanical modelling of folding versus faulting in brittle-ductile wedges. *J. Struct. Geol.* 31, 369–381.
- Smart, K.J., Krieg, R.D., Dunne, W.M., 1999. Deformation behavior during blind thrust translation as a function of fault strength. *J. Struct. Geol.* 21, 855–874.
- Smart, K.J., Ferrill, D.A., Morris, A.P., 2010. Geomechanical modeling of an extensional fault-propagation fold: big brushy canyon monocline, Sierra Del Carmen, Texas. *Am. Assoc. Pet. Geol. Bull.* 94, 221–240.
- Smart, K.J., Ferrill, D.A., Morris, A.P., 2009. Impact of interlayer slip on fracture prediction from geomechanical models of fault-related folds. *Am. Assoc. Pet. Geol. Bull.* 93, 1447–1458.
- Smart, K.J., Ferrill, D.A., Morris, A.P., McGinnis, R.N., 2012. Geomechanical modeling of stress and strain evolution during contractional fault-related folding. *Tectonophysics* 576–577, 171–196.
- Stanton, H.I., Erslev, E.A., 2002. Sheep mountain: back limb tightening and sequential deformation in the Bighorn Basin, Wyoming. *Wyoming Geol. Assoc. Guidebook* 54, 75–87.
- Stockmal, G.S., Beaumont, C., Nguyen, M., Lee, B., 2007. Mechanics of thin-skinned fold-and-thrust belts: insights from numerical models. In: Sears, J.W., Harms, T.A., Evenchick, C.A. (Eds.), *Whence the Mountains? Inquiries into the Evolution of Orogenic Systems: a Volume in Honor of Raymond A. Price*. Geological Society of America, pp. 63–98. Special Paper 433.
- Strayer, L.M., Hudleston, P.J., 1997. Numerical modeling of fold initiation at thrust ramps. *J. Struct. Geol.* 19, 551–566.
- Strayer, L.M., Hudleston, P.J., Lorig, L.J., 2001. A numerical model of deformation and fluid-flow in an evolving thrust wedge. *Tectonophysics* 335, 121–145.
- Strayer, L.M., Suppe, J., 2002. Out of plane motion of a thrust sheet during along-strike propagation of a thrust ramp: a distinct element approach. *J. Struct. Geol.* 24, 637–650.
- Strayer, L.M., Erickson, S.G., Suppe, J., 2004. Influence of growth strata on the evolution of fault-related folds – distinct-element models. In: McClay, K.R. (Ed.), *Thrust Tectonics and Hydrocarbon Systems*, American Association of Petroleum Geologists Memoir 82, pp. 413–437.
- Suppe, J., 1983. Geometry and kinematics of fault-bend folding. *Am. J. Sci.* 283, 684–721.
- Suppe, J., Medwedeff, D.W., 1990. Geometry and kinematics of fault propagation folding. *Am. Assoc. Pet. Geol. Bull.* 83, 409–454.
- Suppe, J., Chou, G.T., Hook, S.C., 1992. Rates of folding and faulting determined from growth strata. In: McClay, K.R. (Ed.), *Thrust Tectonics*. Chapman and Hall, London, pp. 105–122.
- Suppe, J., Connors, C.D., Zhang, Y., 2004. Shear fault-bend folding. In: McClay, K.R. (Ed.), *Thrust Tectonics and Hydrocarbon Systems*, American Association of Petroleum Geologists Memoir 82, pp. 303–323.
- Thomas, A.L., 1993. Poly3D: a Three-dimensional, Polygonal Element, Displacement Discontinuity Boundary Element Computer Program with Applications to Fractures, Faults, and Cavities in the Earth's Crust. M.S. thesis. Stanford Univ., Stanford, Calif.
- Thornton, C., Barnes, D.J., 1986. Computer simulated deformation of compact granular assemblages. *Acta Mechanica* 64, 45–61.
- Timoshenko, S.P., Goodier, J.N., 1970. *Theory of Elasticity*. McGraw-Hill, New York.
- Ting, J.M., Khwaja, M., Meachum, L., Rowell, J., 1993. An ellipse-based discrete element model for granular materials. *Int. J. Numer. Anal. Methods Geomech.* 17, 603–623.
- Trent, B.C., Margolin, L.G., Cundall, P.A., Gaffney, E.S., 1987. The micromechanics of cemented granular material. In: *Constitutive Laws for Engineering Materials: Theory and Applications*. Elsevier, Amsterdam, pp. 795–802.
- Upton, P., 1998. Modelling localization of deformation and fluid flow in a compressional orogen: implications for the Southern Alps of New Zealand. *Am. J. Sci.* 298, 296–323.
- Vanbrabant, Y., Jongmans, D., Hassani, R., Bellino, D., 1999. An application of two-dimensional finite-element modelling for studying the deformation of the Variscan fold-and-thrust belt (Belgium). *Tectonophysics* 309, 141–159.
- Verhooseel, C.V., Scott, M.A., de Borst, R., Hughes, T.J.R., 2010. An isogeometric approach to cohesive zone modeling. *Int. J. Numer. Methods Eng.* 87, 336–360.
- Vietor, T., 2003. Numerical simulation of collisional orogeny using the distinct element technique. In: Konietzky, H. (Ed.), *Numerical Modeling in Micro-mechanics via Particle Methods*. A.A. Balkema Publishers, Lisse, pp. 295–301.
- Walton, O.R., 1984. Numerical simulation of inelastic, frictional particle-particle interactions. In: Roco, M.C. (Ed.), *Particulate Two-phase Flow*. Butterworth-Heinemann, Boston, pp. 884–911.
- Wilkins, S.J., 2007. *Fracture intensity from geomechanical models: application to the Blue Forest 3D survey, Green River Basin, Wyoming, USA*. *Geol. Soc. Lond. Spec. Pub.* 292, 137–157. <http://dx.doi.org/10.1144/SP292.8>.
- Willemsse, E.J.M., Pollard, D.D., Aydin, A., 1996. Three-dimensional analysis of slip distributions on normal fault arrays with consequences for fault scaling. *J. Struct. Geol.* 18, 295–310.
- Williams, J.R., Pentland, A.P., 1991. *Superquadrics and Model Dynamics for Discrete Elements in Concurrent Design*. Technical Report Order No. IESL91–12. Intelligent Engineering Systems Laboratory, Massachusetts Institute of Technology.
- Wissing, S.B., Pfiffner, O.A., 2003. Numerical models for the control of inherited basin geometries on structures and emplacement of the Klippen nappe (Swiss Prealps). *J. Struct. Geol.* 25, 1213–1227.
- Wriggers, P., 2002. *Computational Contact Mechanics*. Wiley, Chichester.
- Yamada, Y., Matsuoka, T., 2005. Digital sandbox modeling using distinct element method: applications to fault tectonics. In: Sorkhabi, R., Tsuji, Y. (Eds.), *Faults, Fluid Flow, and Petroleum Traps*, American Association of Petroleum Geologists Memoir 85, pp. 107–123.
- Zhang, J., Morgan, J.K., Gray, G.G., Harkins, N.W., Sanz, P.F., Chikichev, I., 2013. Comparative FEM and DEM modeling of basement-involved thrust structures, with application to Sheep Mountain, Greybull area, Wyoming. *Tectonophysics* 608, 408–417.
- Zienkiewicz, O.C., Taylor, R.L., Zhu, J.Z., 2005. *The Finite Element Method: Its Basis and Fundamentals*. Butterworth-Heinemann.